

Special Section:

Quantifying the emission, properties, and diverse impacts of wildfire smoke

Key Points:

- Modeling and satellite observations of smoke
- Smoke impacts on the atmospheric radiation and clouds
- Provides recommendations for the future research

Correspondence to:

I. N. Sokolik,
isokolik@eas.gatech.edu

Citation:

Sokolik, I. N., Soja, A. J., DeMott, P. J., & Winker, D. (2019). Progress and challenges in quantifying wildfire smoke emissions, their properties, transport, and atmospheric impacts. *Journal of Geophysical Research: Atmospheres*, 124, 13,005–13,025. <https://doi.org/10.1029/2018JD029878>

Received 29 NOV 2018

Accepted 26 SEP 2019

Accepted article online 22 OCT 2019

Published online 8 DEC 2019

Author Contributions:

Conceptualization: A. J. Soja, D. Winker
Formal analysis: A. J. Soja, D. Winker
Methodology: A. J. Soja, D. Winker
Validation: A. J. Soja, D. Winker
Writing – review & editing: A. J. Soja, D. Winker

Progress and Challenges in Quantifying Wildfire Smoke Emissions, Their Properties, Transport, and Atmospheric Impacts

I. N. Sokolik¹ , A. J. Soja^{2,3} , P. J. DeMott⁴ , and D. Winker³

¹School of Earth and Atmospheric Sciences, Georgia Institute of Technology, Atlanta, GA, USA, ²National Institute of Aerospace, Hampton, VA, USA, ³NASA Langley Research Center, Hampton, VA, USA, ⁴Department of Atmospheric Science, Colorado State University, Fort Collins, CO, USA

Abstract Wildfire is a natural and integral ecosystem process that is necessary to maintain species composition, structure, and ecosystem function. Extreme fires have been increasing over the last decades, which have a substantial impact on air quality, human health, the environment, and climate systems. Smoke aerosols can be transported over large distances, acting as pollutants that affect adjacent and distant downwind communities and environments. Fire emissions are a complicated mixture of trace gases and aerosols, many of which are short-lived and chemically reactive, and this mixture affects atmospheric composition in complex ways that are not completely understood. We present a review of the current state of knowledge of smoke aerosol emissions originating from wildfires. Satellite observations, from both passive and active instruments, are critical to providing the ability to view the large-scale influence of fire, smoke, and their impacts. Progress in the development of fire emission estimates to regional and global chemical transport models has advanced, although significant challenges remain, such as connecting ecosystems and fuels burned with dependent atmospheric chemistry. Knowledge of the impact of smoke on radiation, clouds, and precipitation has progressed and is an essential topical research area. However, current measurements and parameterizations are not adequate to describe the impacts on clouds of smoke particles (e.g., CNN, INP) from fire emissions in the range of representative environmental conditions necessary to advance science or modeling. We conclude by providing recommendations to the community that we believe will advance the science and understanding of the impact of fire smoke emissions on human and environmental health, as well as feedback with climate systems.

1. Introduction

Smoke is composed of airborne liquid and solid particulates and gases that are emitted when fuels undergo combustion or burning. Additionally, the turbulence and buoyancy associated with a fire front results in entrainment of soil minerals and organic matter into smoke plumes, which enhances mass concentrations of soil tracer species (Kavouras et al., 2012; Maudlin et al., 2015; Schlosser et al., 2017). The composition of particles and gases emitted from fires are dependent on the fuel type, temperature, and conditions of combustion (Akagi et al., 2011; Meinrat O. Andreae & Merlet, 2001; Cruz et al., 2018; Duff et al., 2017; Kukavskaya et al., 2012; Soja et al., 2004). High temperatures, dry fuels, and more complete combustion lead to increased emissions of carbon dioxide (CO_2), ash, water vapor, nitrogen oxides (NO_x), and sulfur dioxides (SO_2). In contrast, partial oxidation of fuels leads to increasing hazardous emissions, such as carbon monoxide (CO), hydrogen sulfide (H_2S), hydrogen cyanide (HCN), and ammonia (NH_3). Smoke also interacts with other atmospheric trace gases and undergoes photochemical processing as smoke is transported and evolves over time. Although the processes are not fully understood, photochemical processing includes the rapid conversion of short-lived reactive trace gases and the production of ozone and secondary organic aerosol. While the factors that influence smoke chemistry are daunting, there are continuing and current satellite missions and field campaigns that hold promise to address some of the challenges and controversies: the 2018 NSF Western wildfire Experiment for Cloud chemistry, Aerosol absorption and Nitrogen (WE-CAN) airborne campaign; the combined NASA/NOAA Fire Influence on Regional and Global Environments Experiment–Air Quality (FIREX-AQ) airborne campaign; Cloud, Aerosol, and Monsoon Processes Philippines Experiment (CAMP2Ex); and the launch of NASA's TEMPO (Tropospheric Emissions: Monitoring Pollution) mission in the 2019–2021 time frame,

which will complement two additional geostationary satellites tracking air pollution (GEMS covering Southeast Asia and the European Sentinel-4).

Smoke aerosols, that is, particles that have been emitted directly from wildfires or formed from gaseous precursors in the atmosphere after their emission from wildfires, play a multifaceted and important role in the environment and the climate system in general. Large and extreme natural fires burn as a result of persistent high-pressure systems, which results in dry fuels and minimal associated near-field precipitation. The size of emitted smoke particles is wide-ranging, and larger particles are often deposited in the near-field (1–2 km). Small particles injected high in the atmosphere can remain for weeks to months, even reaching the lower stratosphere, where long-term climate effects are possible (Fromm et al., 2010). Recently, David A Peterson et al. (2018) argued the mass of aerosols injected into the lower stratosphere from extreme fires burning in western North America were equivalent to a moderate volcanic eruption, and a full season of perturbations from fire could significantly perturb the stratosphere. Smoke plumes can be transported over long distances, affecting large areas downwind of wildfires, and smoke plumes have been observed to circumnavigate the Earth (Damoah et al., 2004). Removal mechanisms include nucleation and impaction scavenging, rainout, and wash out. However, heavy smoke was shown to inhibit the onset of precipitation, which has implications for hydrologic cycles (Meinrat O Andreae et al., 2004). Also, because precipitation is a major smoke removal mechanism, the lack of precipitation leads to a longer atmospheric lifetime and long-range transport (Lu & Sokolik, 2013).

Once in the atmosphere, smoke aerosol interacts with and alters solar radiation fields, which leads to multiple and complex impacts. The radiative forcing of fire emissions plays a significant global role in both natural and anthropogenic climate perturbations, with large changes in radiative forcing of smoke emissions between preindustrial and present-day conditions (D S Ward et al., 2012). By interacting with the ultraviolet (UV) component of solar radiation, smoke affects the photolysis rates of major photochemically formed species, such as ozone. Furthermore, smoke has a significant impact on the surface radiation budget, affects the profile of heating rates through the atmosphere, and alters the radiative forcing at the top of the atmosphere (TOA). Smoke particles deposited on snow and ice can change snow reflectivity, which affects surface albedo, the radiation balance, and can result in rapid increases in snow and ice melting (Keegan et al., 2014; Polashenski et al., 2015; J L Ward et al., 2018). Smoke from boreal (Canada, Alaska, Siberia) and lower latitude ecosystems can be transported northward, encircling the Earth, and deposited on snow- and ice-covered surfaces (Natarajan et al., 2012; Thomas et al., 2017), which can heighten the presence of in-snow and atmospheric aerosol effects. The overall impact of smoke on radiative fields makes it an important climatic agent, even though our understanding of the direct and indirect mechanisms, extent, and interacting effects on the radiation balance are not fully understood or accounted for in models.

Wildfire can cause substantial property damage and loss of life. Smoke from fire statistically increases hospital visits that directly include increases in respiratory (asthma, pneumonia, acute bronchitis) and cardiopulmonary symptoms, heart failure, and death (Rappold et al., 2011). In the greater Moscow region in Russia in 2010, the Munich reinsurance company estimated 56,000 people died due to the extreme heat and smoke that enveloped this populated region (primarily in drained peatlands; cost \$630 M; Writer, 2015). Under the control of weather and climate, each year, fires are reported to be increasingly catastrophic (deadliest, costliest, largest), and every year surpasses the previous. For example, in 2017, a series of wildfires in Chile were reported as the “worst” in modern Chilean history; Portugal experienced catastrophic fires that resulted in 66 fatalities (globally ranked 11th deadliest in the last 100 years); Montana experienced its most expensive fire season; British Columbia, Canada (CAN) reported its largest burned area; and California (CA) experienced its most expensive and largest fire in CA history (Thomas fire). Then, in 2018, the unusually long European heat wave resulted in reports of the “Arctic on Fire” in Sweden, and Greece experienced another deadly fire season (99 fatalities; second deadliest in the twenty-first century, globally ranked fourth deadliest in the last 100 years). Also in 2018, the reported “historic” largest fire seasons in CAN and CA were surpassed (CA: Mendocino Complex largest in CA history; Camp fire globally ranked the fifth deadliest in last 100 years). These are critical subjects that are the driving force behind this work, but a full assessment of ecosystem-human health and fire-weather-climate feedback are beyond the scope of this review. We do endeavor to incite the science and understanding that will lead to improved air quality and a population informed as to the connections between weather, climate, ecosystems, and fire regimes.

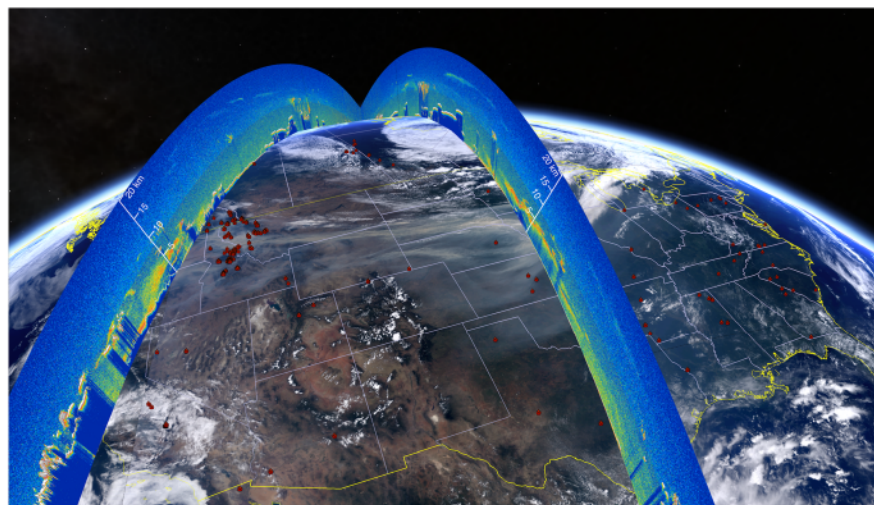


Figure 1. Smoke extends across the United States 4 September 2017 (figure attributable to Roman Kowch). A MODIS Terra visible image is overlaid with two vertical CALIOP lidar tracks showing the vertical and horizontal extent of this smoke plume, which is circumnavigating the Earth. CALIOP data provide the unique vertical structure of smoke, and these data show the smoke hovering around 5 km, ranging from the surface to the boundary layer to about 9 km. Together these satellite data highlight both the horizontal and vertical influence of smoke-laden surface pollution and elevated smoke transport.

This special issue “Quantifying the emission, properties, and diverse impact of wildfire smoke” and this review are focused on summarizing progress in our understanding of smoke emissions and transport, the satellite data that are available to characterize smoke, and the diverse impacts of smoke on the atmosphere and related climate system. The paper is organized as follows. Section 2 presents a summary of satellite data available for observing fire and smoke, while section 3 summarizes progress in quantifying smoke emissions. Section 5 focuses on the radiative impacts of smoke, and section 6 discusses the impacts of smoke on clouds and precipitation. Section 6 provides a summary and recommendations to encourage future research directions.

2. Observation and Current Quantification of Fire and Smoke From Satellites

Satellite remote sensing provides a unique and powerful way to observe the full horizontal and vertical extent of fire and the transport of smoke plumes (Figure 1). Fire and smoke emissions and transport can be quantified, regionally and globally, from a safe distance using satellite data and information. Polar orbiters with a large swath width typically provide a one-day and one-night view of the Earth at a moderate resolution, so these satellites have generally been used to explore the dynamic large-scale connections between the Earth, fire, and intercontinental smoke transport and deposition. Geostationary satellites provide a continuous hemispheric view of the Earth, and they have historically provided information at a high-temporal resolution (~30-min data) at the expense of spatial resolution. Due to recently improved spatial resolution and global availability, geostationary satellites are becoming increasingly valuable for assessing active fires, air quality, and emissions inventories (e.g., GOES-16, 2 km \times 2 km).

Both passive and active remote-sensing techniques have been used to study smoke properties, as well as fire sources and atmospheric transport. Passive sensors have been invaluable for viewing and characterizing fire regimes (e.g., healthy and unhealthy vegetation, active fire, burned area, fire severity, burning vegetation, fire weather, and potential change) and the horizontal transport and circumnavigation of smoke. A global long-term passive data set of fire and smoke has existed since 1978, when NOAA launched the meteorological satellite TIROS-N with the Advanced Very High Resolution Radiometer (AVHRR) instrument onboard, which unexpectedly proved to be instrumental in detecting active fires and defining burned areas from space (Cahoon et al., 1992; Smith & Rao, 1971). Currently, two Moderate Resolution Imaging Spectroradiometer (MODIS) instruments onboard NASA’s Terra (morning overpass) and Aqua (afternoon overpass) satellites

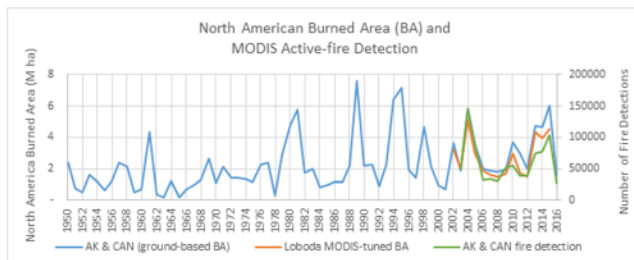


Figure 2. Comparison of long-term, ground-based official statistics to satellite-based burned area (BA) and active-fire detection data. Ground-based data are provided by Alaskan and National Interagency Coordination Centers and the Canadian Wildland Fire Information System. The regionally optimized MODIS-based BA algorithm provides estimates that compare best to ground-based data, demonstrating the capability of satellite data to accurately assess BA (Loboda et al., 2011). In addition, MODIS fire detections (Terra and Aqua, v6.1) track well with burned area. In this region, as in many others, the number of fire detections does not directly equate to BA by assuming a 1 to 1-km² BA (e.g., ~100,000 detection in 2015 = 10 Mha, which is too high).

smoke emissions, smoke transport, air quality, and potential changes in fire regimes. Long-term data records exist in some regions (Figure 2), which provide a means for verification and validation of satellite data, but these long-term data sets do not exist in most of the world. In fact, across the circumboreal, there is already evidence of climate-induced change in fire regimes (Kasischke & Turetsky, 2006; Partain et al., 2016; Soja et al., 2007). Comparing the first 33 years of the North American boreal data record to the recent 33-year data record shows an increase of about 42% in burned areas. In the United States, over the 39 years from 1960 to 1999, burned area exceeded 7 M acres only once in 1963. In contrast, from 2000 to 2018, burned area exceeded 7 M acres 11 times, reaching >9 M acres in five of these years (2006, 2007, 2012, 2015, and 2017; National Interagency Fire Center data; <https://www.nifc.gov/>). Regions across the world are reporting unprecedented fires (Australia Black Saturday 2009, 2015; Texas, Ireland, United Kingdom 2011; Russia 2010, 2015; Europe Mediterranean wildfires 2009, 2017, 2018; South Korea 2000, 2013; Indonesia 1997, 2015).

Assessing fire regimes globally and regionally is complex, complicated by regional, ecosystem, and fire weather differences, as well as the human factors that can dominate in many regions. Globally, based on

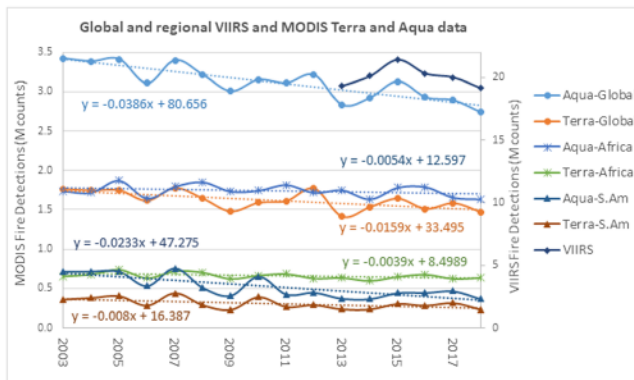


Figure 3. Comparison of the long-term VIIRS and MODIS fire-detection data products (first full year of Terra and Aqua 2003). The Aqua afternoon overpass consistently accounts for about 43% more fire detections than the Terra morning overpass. Africa accounts for the greatest number of fire detections with South American (S.Am) accounting for the second greatest number. The largest decrease in fire detections since 2003 is in South America, followed by decreases in Africa, which account for the majority of the global decrease in fire detections. VIIRS 375-m data contain an order of magnitude more fire detections than both MODIS products combined.

provide active-fire detection (thermal anomaly), burned area (BA), Fire Radiative Power (FRP), and Aerosol Optical Depth (AOD) measurements (Giglio et al., 2003; Giglio et al., 2006; Justice et al., 2002; D.P. Roy et al., 2008; Sayer et al., 2014). In addition, the Multi-angle Imaging SpectroRadiometer (MISR) also observes smoke optical depth (Kahn & Gaitley, 2015). The next generation of environmental satellites is part of the interagency NASA/NOAA Joint Polar Satellite System (JPSS) global observing system. The Visible Infrared Imaging Radiometer Suite (VIIRS) instrument onboard both Suomi National Polar-orbiting Partnership (S-NPP—launched 2011) and NOAA-20 (launched 2017) have the capability to provide enhanced high-resolution fire detection, FRP, burned area, and Aerosol Optical Thickness (AOT) data (M. Li, et al., 2018; Schroeder et al., 2014).

Climate-induced change in patterns of fire and fire regimes (e.g., increases in length of fire season, fire severity, fire weather, burned area) are predicted, particularly in Northern-Hemisphere upper latitudes (Flannigan et al., 2009; Stocks et al., 1998; Westerling et al., 2006), so understanding past and present fire regimes and their feedback is critical. Currently, satellite data are able to accurately evaluate regional and global patterns of fire,

smoke emissions, smoke transport, air quality, and potential changes in fire regimes. Long-term data records exist in some regions (Figure 2), which provide a means for verification and validation of satellite data, but these long-term data sets do not exist in most of the world. In fact, across the circumboreal, there is already evidence of climate-induced change in fire regimes (Kasischke & Turetsky, 2006; Partain et al., 2016; Soja et al., 2007). Comparing the first 33 years of the North American boreal data record to the recent 33-year data record shows an increase of about 42% in burned areas. In the United States, over the 39 years from 1960 to 1999, burned area exceeded 7 M acres only once in 1963. In contrast, from 2000 to 2018, burned area exceeded 7 M acres 11 times, reaching >9 M acres in five of these years (2006, 2007, 2012, 2015, and 2017; National Interagency Fire Center data; <https://www.nifc.gov/>). Regions across the world are reporting unprecedented fires (Australia Black Saturday 2009, 2015; Texas, Ireland, United Kingdom 2011; Russia 2010, 2015; Europe Mediterranean wildfires 2009, 2017, 2018; South Korea 2000, 2013; Indonesia 1997, 2015).

Assessing fire regimes globally and regionally is complex, complicated by regional, ecosystem, and fire weather differences, as well as the human factors that can dominate in many regions. Globally, based on MODIS thermal anomaly data from 2003 to 2018, we find a global decrease in fire, which is largely driven by decreased burning in South America and Africa (Figures 3 and 4). This result is consistent with Andela et al. (2017), who reported decreases in burned area from 1998 to 2013, particularly in savannas, cerrados, and grasslands where agricultural expansion and intensification are the dominant drivers of change. In South America, active measures at federal, state, and local levels have resulted in a decrease in the rate of deforestation in the Amazon forest in Brazil, although the rate of deforestation and fire is still significant and disconcerting. An Integrated Fire Management program was reported in three protected areas in Brazil that actively manages fire and decreases the proportion of areas burnt by late-dry season wildfires, resulting in major advances in cerrado management and conservation (Schmidt et al., 2018). Additionally, Aragão and Shimabukuro (2010) showed fire-free land-management can reduce fire incidence by as much as 69%. Over the last two decades, there is evidence to support a global decrease in fire in human-dominated landscapes in regions that promote agricultural practices or fire management that reduces fire. However, currently in Brazil (2019), human fire ignitions have increased in comparison to recent years in the Amazonian basin, which is a tropical forest that evolved with negligible fires over millennia. Unlike temperate and

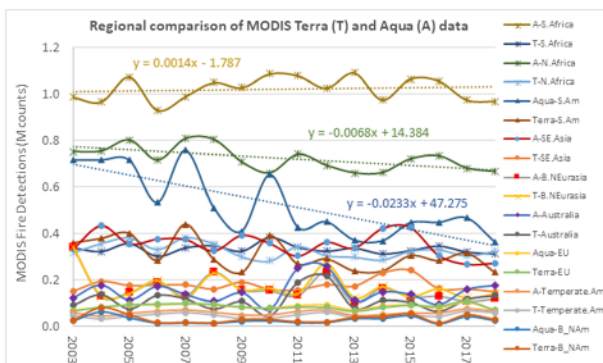


Figure 4. Comparison of the long-term MODIS fire-detection data. Regionally, the Aqua afternoon overpass accounts for the greatest number of fire detections, with the exception of boreal (B) regions, which is likely due to cloud cover and overlapping overpasses at high latitudes; boreal fires peak in the late afternoon. The largest decreasing trend is in the Aqua South America data, followed by Aqua North Africa; Aqua South Africa shows a slight increasing trend since 2003. Fire detection data do not account for total burned area or the depth of burn, both of which are critical to estimating the total mass of fuel burned and fire emissions.

trend, one that is incorrect when viewed over a longer time frame (Figure 2). To mitigate and/or advance our understanding of the catalyst that drive fire, long-term data records and a consideration of the regional factors controlling fires are necessary, whether human- or climate-induced.

Satellite results, shown in Figures 3 and 4, demonstrate that the Aqua afternoon overpass consistently detects about 43% more fires than the Terra morning overpass (Figures 3 and 4), which should be a consideration when analyzing data and establishing overpass times for new satellites. For example, Giglio et al. (2006) developed a correlation to relate Terra-only active-fire data to total burned areas, so using this correlation factor for all Aqua and Terra detection data would result in a gross overestimate of burned areas, yet this is used. Time of day directly impacts fire analyses and emissions accounting. For instance, agricultural and prescription fires typically burn when conditions are best to maintain fire control and achieve prescription objectives [morning (dew burn off)/late afternoon (before sunset); relatively lower temperatures (T) and relatively higher relative humidity (RH)]. On the other hand, natural fires peak in the late afternoon, when T is highest, RH is lowest, and fuels are the driest (available and ready to burn). One exception in the fire-detection data is in the high-northern-latitude boreal regions, where the morning Terra data are approximately equivalent to or surpass the number of Aqua fire detections. However, boreal fire regimes peak in the late afternoon; therefore, this morning-overpass discrepancy could be due to (1) thick cloud and smoke cover inhibiting detections in the late afternoon and (2) overlapping polar overpasses at high latitudes before clouds and thick smoke columns develop.

Known as the fire continent, Africa contributes the largest number of fire detections (Figures 3 and 4). However, peatlands and the deep soil organic matter stored in boreal regions and Indonesia contribute the largest depths of carbon consumed (meters). The enhanced VIIRS 375-m active-fire product reports about 4.5 times the number of active fires than the combined Terra and Aqua MODIS 1-km products, which presents challenges and benefits to the communities assessing long-term fire data, changes in fire regimes, and to those that manage fires. Relatively speaking, our global fire and emissions record is short, which argues for the necessity of a long-term satellite data record.

The main aerosol optical property retrieved from passive satellite observations is optical depth, and AOD provides a consistent measurement, which has been successfully used to characterize smoke and other aerosols (e.g., dust) for decades. However, passive sensors may categorize near-field smoke from large fires as clouds, so that AOD from large and extreme fires is missing, until it is transported, diffused, and then the smoke is recognized downwind (Mhawish et al., 2019). Retrievals of additional properties such as the Angstrom exponent or the fine mode fraction of optical depth can be used to infer the presence of smoke over water. Passive satellite sensors rely on look-up tables to retrieve aerosol optical properties. Look-up tables

boreal forests, which have evolved with fire and experienced glaciations, the nutrients stored in these tropical forests are stored in the aboveground vegetation, so these forests will not recover.

At the same time, there is evidence that supports the preponderance of climate-induced fire regime change across landscapes, particularly when considering long-term and regionally comprehensive investigations. Jolly et al. (2015) used several fire weather indices from 1979 to 2013 to show a global increase in the frequency of long fire weather seasons, which coincide with long and large fire seasons, and they showed a doubling of the area affected. In a regional investigation, despite the influence of suppression across the western United States, several investigations have concluded increases in burned area across the west in the twentieth century were controlled by climate (Littell et al., 2009; Westerling et al., 2006). Additionally, Littell et al. (2009) argued that the differences in ecosystems underscore the need to consider ecological context (vegetation, fuels, and seasonal climates) to identify specific drivers of burned area. Furthermore, in this work, a slight decrease in the fire trend in boreal North America is evident in both Aqua and Terra thermal anomaly data (Figure 4). However, when placed in the longer-term context from ground-based records, this is a short-term deviation from the long-term

include assumptions on aerosol microphysical properties, which are used to precalculate the signals that would be observed by a satellite sensor in a particular smoke-laden condition. Thus, retrievals are possible only within a predefined space of parameters, and the accuracy and uniqueness of the retrievals need to be validated. Independent measurements of the aerosol optical depth, that is, from ground-based Sun photometer measurements, are often used as part of the validation procedure. While ground-based Sun photometers make direct and accurate measurements of optical depth (unitless), observations of different parts of the atmosphere, differences in viewing geometry, wavelengths, and in time and space between the satellite and ground-based observations, can all introduce uncertainties.

Currently, there are two satellite instruments that are capable of statistically characterizing the vertical height and vertical extent of smoke and aerosols in the atmosphere, the Multi-angle Imaging SpectroRadiometer (MISR) instrument onboard the Terra satellite and the Cloud-Aerosol Lidar with Orthogonal Polarization (CALIOP) onboard the Cloud-Aerosol Lidar and Infrared Pathfinder Satellite Observation (CALIPSO). MISR uses stereographic heights to estimate near-field smoke plume injection height (Kahn et al., 2007; Kahn et al., 2008), and MISR hosts a well-developed database of plume heights in a variety of ecosystems (Val Martin et al., 2012). However, these data tend to underestimate plume injection height for two reasons: (1) the MISR product is produced from morning only data and fires peak in late afternoons when temperatures are highest and relative humidity is lowest; and (2) large fire plumes typically lack distinct boundaries, which is required to estimate smoke or cloud heights using stereographic views. Mardi et al. (2018) characterized 81 smoke plumes over two years during in situ airborne sampling and found that most of the smoke was resident in free troposphere, not below the boundary layer, which has further implications for feedback with clouds.

Lidar remote sensing is fundamentally different from remote sensing with passive sensors. Active lidar carries its own light source and is able to detect and characterize aerosol layers at night as well as during the day. Lidar senses the scattering of a short laser pulses as they propagate through the atmosphere, allowing vertically resolved retrievals of aerosol extinction down to the Earth's surface. Polarization-sensitive lidar, such as CALIOP, discriminates cloud layers from smoke and dust aerosols—the two aerosol types typically found in the free troposphere. Whereas the primary aerosol parameter retrieved by passive sensors is optical depth, for lidar it is the vertically resolved profile of aerosol extinction (Z Y Liu et al., 2009; Omar et al., 2009; Winker et al., 2010). Lidar retrievals require an estimate of the ratio of aerosol extinction to 180-degree backscatter, referred to as the lidar ratio, rather than look-up tables or radiative transfer calculations. While the lidar ratio depends on the aerosol size, composition, and shape, in practice it was found to be relatively invariant for transported smoke (Z Liu et al., 2015).

CALIOP lidar data have been used to define the vertical extent of smoke plumes through the atmosphere. Opportunities to validate CALIOP extinction profiles are limited due to the narrow swath width; nevertheless, AOD Sun photometer measurements and profiles from airborne High Spectral Resolution Lidar (HSRL; Rogers et al., 2014) and in situ profiling (Sheridan et al., 2012) have been useful. In general, lidar is more sensitive to relatively transparent smoke layers than passive sensors, and the HSRL instrument has shown a demonstrated ability to distinguish both near- and far-field smoke plumes (Burton et al., 2012). When paired with a back-trajectory model, CALIOP data have been used to define smoke detrainment height and the evolution of smoke plumes over a day (Soja et al., 2012). Using near-field and far-field plume heights from MISR and CALIOP, respectively, Raffuse et al. (2012) found that model placement of the plume into the correct transport layer was more important to correctly modeling the transport than correctly modeling the plume injection height at the fire location. Together, MISR and CALIOP have the potential to produce the statistics necessary to improve Chemical Transport and climate model parameterization and verify modeled plume injection height, thus substantially improving fire emission transport, air quality, and feedback with climate systems.

3. Characterization of Smoke Emissions

Emissions from fires are affected by a wide variety of factors that include fuel conditions [ecosystem type and mass (e.g., age/succession and geology), structure, and moisture content], and fire weather (cumulative temperature, relative humidity, wind speed, and precipitation), which drive fire intensity, and in turn, these can be rapidly and heterogeneously modified by fires as they burn. Smoke emission estimates have traditionally

been based on a bottom-up approach. The majority of the smoke emission models are built on a book-keeping mass-accounting technique (Seiler & Crutzen, 1980), in which the mass of smoke emissions (M ; kg) is expressed as

$$M = a \cdot \alpha \cdot \beta \cdot EF \quad (1.1)$$

where a is the burned area (m^2), α is the amount of biomass fuel (kg carbon/ m^2), β is the combustion fraction (unitless), and EF is the emission factor for gases and particulate matter or species-specific aerosol component emissions (kg/kg carbon). Over the life of a fire, different combinations of flaming and smoldering combustion lead to time-varying emissions that influence plume rise and detrainment, subsequent transport, and the chemical evolution of smoke. The fraction of flaming to smoldering emissions is a significant ratio, because flaming emissions are more efficient resulting in characteristically different smoke [highly oxidized simple molecules H_2O , CO_2 , N_2 , NO , BC (black carbon)]; whereas, smoldering is less efficient and less healthy, releasing relatively more CO , H_2S , HCN , NH_3 , NMHC (nonmethane hydrocarbons), and primary OC (organic carbon) aerosols (Akagi et al., 2011; Meinrat O. Andreae & Merlet, 2001). Developments in remote-sensing instruments (AVHRR, GOES, MODIS, VIIRS, etc.), products, and fire retrieval algorithms since the 1980s (Dozier, 1981; Giglio et al., 2003; Prins & Menzel, 1992) make it feasible to estimate burned area and smoke emissions at regional and global scales over almost four decades.

There are three unique fire products that can be used to generate burned area (BA): burn scars, active-fire detection, and FRP. The first “burn scar” type (MODIS MCD45) is based on changes in surface reflectance and is optimized for the tropics and savannahs (D.P. Roy et al., 2005). MODIS MCD64 uses a combination of active fire with a vegetation index and is optimized for northern forests (Giglio et al., 2009). Advantages of the burn scar product are (1) the postburn, cloud-free area is reported and (2) no additional assumptions are needed to apply BA (Petrenko et al., 2012; Randerson et al., 2012; Roberts et al., 2011). However, in this type of product, small fires are often missed and the uncertainty associated with the date of burn is too large for mesoscale modeling (± 8 days; Randerson et al., 2012). A fire emission inventory based on these data is the Global Fire Emissions Database (GFED; Randerson et al., 2012; van der Werf et al., 2017).

The second product type, “active fire,” is derived from the spectral signature of fire in midinfrared channels (Dozier, 1981; Giglio et al., 2016). A global fire emission inventory based on MODIS active fire is the Fire INventory from NCAR (FINN; Wiedinmyer et al., 2011). Geostationary satellites are increasingly being used to develop national fire emission inventories. Derived from the observations of GOES satellites, the WildFire Automated Biomass Burning Algorithm (WF_ABBA) product reports the instantaneous estimation of sub-pixel fire sizes with high-temporal resolution (15–30 min) but relatively low-spatial resolution, especially for high latitudes ($4\text{ km} \times 4\text{ km}$ at nadir; Prins et al., 1998). However, the recently activated GOES-16 satellite offers improved temporal and spatial resolution ($2\text{ km} \times 2\text{ km}$). When previously applying the WF_ABBA product in modeling extreme wildfire events, many studies significantly underestimated smoke emissions by 5 to 10 times, as compared to aerosol optical depth (AOD) observations (Lu & Sokolik, 2013; O'Neill et al., 2006; Reid et al., 2009; Wu et al., 2011), and Al-Saadi (2009) found underestimates between 62 and 77% when compared to a ground-based data set.

The other three factors (α , β , EF) in equation (1.1) are dependent on the preceding fire-weather conditions and the vegetation amount (carbon fuel) and structure, which all act to fuel the fire. On a large scale, each ecosystem type contains a total amount of fuel (α), and the amount of fuel that is dry enough to burn is under the control of weather and fuel size (β). The Real-time Air Quality Modeling System (RAQMS) was the first large-scale Chemical Transport Model (CTM) to use ecosystem-specific fuels and a proxy for fire weather (Haines index) to determine the fraction of fuel consumed (Petrenko et al., 2012; Pierce et al., 2007; Pierce et al., 2009). Land cover databases are often used to define ecosystems, thus fuels, at the large scale. Models project burned areas on vegetation maps, such as the GLCC (Global Land Cover Characteristic database)v2 used for the FLAMBE (Fire Locating And Monitoring of Burning Emissions) smoke emission inventory (Reid et al., 2009), MODIS IGBP (International Geosphere Biosphere Programme) used for the FINN smoke emission inventory (Wiedinmyer et al., 2011), and GLC2000 (Global Land Cover 2000) used by GOCART (Goddard Chemistry Aerosol Radiation and Transport; Petrenko et al., 2012). The uncertainties associated with these three factors are noticeable, and hamper the accuracy of smoke emission estimates (Langmann et al., 2009). For example, the available biomass fuel in boreal North America can vary by a

factor of 3–20 within a region of limited ecosystem diversity (McKenzie et al., 2007). In Siberia, Soja et al. (2004) found the difference in the amount of biomass/fuel contained between ecosystems can vary by as much as 45%, and the difference between weather-dependent low- and high-severity fires or the actual fuel consumed can be between 80 and 84%. Accounting for differences in ecosystems, severity, and extreme events, available fuel can vary by a factor of 22.

Using a novel approach, Kaufman et al. (1998) and Ichoku and Kaufman (2005) suggested a technique for estimating smoke emissions. In this technique, fire radiative power (FRP) is utilized as a driver for estimating smoke emissions. FRP is retrieved as a function of brightness temperatures in the 4- μm channel. The FRP values from active fires can be obtained from the MODIS or VIIRS active fire products. In this technique, the smoke emission rate of active fire “hot spots” is proportional to the FRP value. The ratio of the smoke emissions to FRP, or the particulate matter emission coefficient (Ce), is a function of vegetation type (Kaiser et al., 2012; Sofiev et al., 2009), as typically defined by regions (Ichoku & Kaufman, 2005). Emission databases that rely on FRP data include the Quick Fire Emissions Dataset (QFED) and the Global Fire Assimilation System (GFAS; Ichoku & Ellison, 2014; Kaiser et al., 2012).

Each of the satellite products and techniques discussed above has its own advantages and limitations in terms of quantitatively estimating smoke emissions. Geostationary satellites are continually overhead and provide valuable high-temporal resolution data, although the spatial resolution of these instruments is lower than polar orbiters. The spatial resolution of MODIS and VIIRS fire products is moderate (375 m to 1 \times 1 km), but their temporal resolution is limited by the satellite’s polar orbit and overpass time (MODIS instruments on both Terra and Aqua satellites; VIIRS on Suomi-NPP and JPSS). Some studies integrate multiple satellite products to generate a more accurate time series of smoke emissions (Freeborn et al., 2011; Giglio et al., 2010; Randerson et al., 2012; Roberts et al., 2011; X Zhang et al., 2011), because using multiple products can compensate for the limitations of individual sensors. To compensate for small fires that are often missed, Randerson et al. (2012) associated fire detections that fall outside of burn scars with small burned areas, but this approach has been shown to introduce significant errors (T Zhang et al., 2018). In another work, X Zhang et al. (2011) used the ratio of high-resolution burned areas (Landsat TM/ETM) to fire detections (AVHRR and MODIS) in an effort to enhance burned area estimates. Efforts have been made to refine the diurnal cycle of fire in some models based on fire science intelligence and using high-temporal resolution geostationary (e.g., WF_ABBA) data. Each of these developments continually strive to advance fire emissions.

Smoke injection height and detrainment is critical in determining the transport of smoke plumes, because the height at which smoke is detained determines its transport and deposition (smoke tends to travel faster and remain in the atmosphere longer at higher altitudes; Myhre et al., 2013; Sessions et al., 2011; Thomas et al., 2017). Smoke can be injected in the boundary layer, in the free troposphere, above the stable layer, or even in the lower stratosphere. Fire-augmented “pyro-cumulus” and “pyro-cumulonimbus” events have been shown to be more common than previously thought (Fromm et al., 2010; David A. Peterson et al., 2017). Smoke tends to be injected at multiple altitudes as numerous smoke-laden anvils, as opposed to single-source smoke stacks, depending on the ambient meteorological conditions, burning phases (flaming or smoldering phases), and fuel conditions (vegetation amount, structure, and moisture content). However, many modeling studies have assumed smoke particles are either emitted to the first layer of the model (e.g., Graf et al., 2009) or to a preset height (e.g., Pfister et al., 2008; Wang et al., 2006). Freitas et al. (2007) developed a physically based plume rise model that can calculate the smoke injection height for several different vegetation types. This plume rise model was coupled to the Regional Atmospheric Modeling System (RAMS; Freitas et al., 2009) and WRF-Chem models (Grell et al., 2011). However, Sessions et al. (2011) demonstrated that the plume rise model is very sensitive to the assumptions about the burned areas.

4. Smoke Radiative Impact

Smoke aerosols strongly interact with UV and solar radiation, but no significant impacts of smoke on infrared radiation are expected due to the small size of smoke particles. Assessments of the diverse radiative impacts of smoke have proven difficult, mainly due to the large variability in smoke loadings and properties. While in the atmosphere, smoke can cause significant impacts to solar and UV fluxes, thus affecting the radiation balance at the top of the atmosphere (TOA) and at the surface (J L Ward et al., 2018). In the

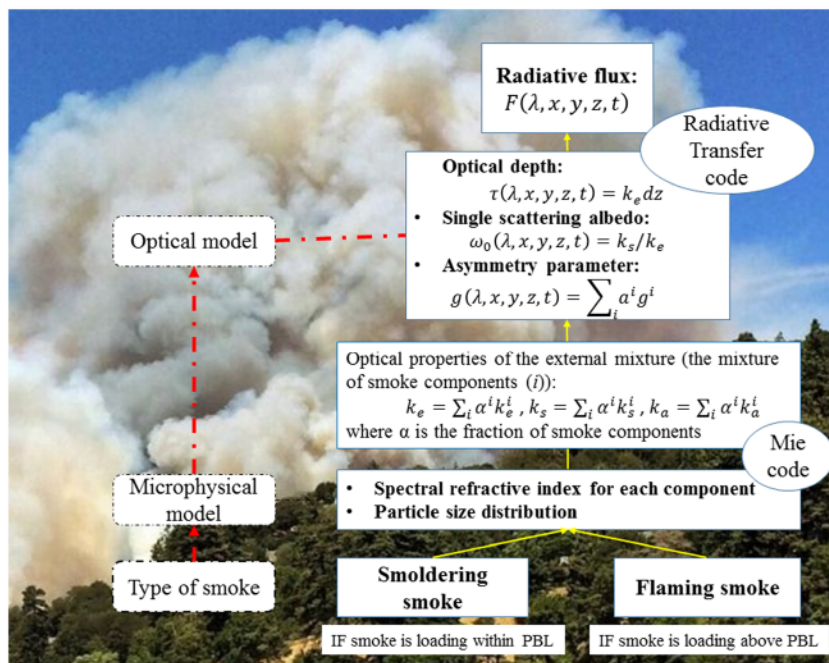


Figure 5. Pictorial showing the steps required to compute radiation in smoke-laden conditions. These are the computations currently used in models to assess the radiative impact of smoke (e.g., WRF-SMOKE). We recognize that smoke emissions are never purely flaming or smoldering.

boundary layer and free troposphere, the profile of heating and cooling can affect atmospheric temperature (Natarajan et al., 2012). Smoke may impact photochemical reactions by altering the actinic fluxes in different spectral ranges that all work to drive photochemistry. Smoke optical properties are determined by the size resolved chemical composition, in particular the presence of black carbon and organic carbon (Laskin et al., 2015).

Figure 5 illustrates the information necessary to compute and model radiative fluxes (e.g., WRF-SMOKE). First, smoke type (flaming versus smoldering), the percentage of each of these, and the layer of the atmosphere to which smoke is injected is required, and these relationships are unique, dependent on fuel type and dryness, and are not fully understood. Next, the size distribution for each emitted aerosol species is required. Then, optical properties are computed for each individual species and the optical properties of the mixture are found by summing the weighted individual properties with the weight assigned to each species present. The profile of optical properties is then used to compute radiative fluxes. This procedure involves several critical assumptions. Particles are typically assumed to be spherical or spheroidal, yet many studies have demonstrated that smoke particles can have nonspherical chain-like shapes (Alexander et al., 2008). A new database of smoke particle shapes, as a function of particle size, as well as burning conditions, could be established to significantly improve the assessment of smoke radiative impacts. Ongoing FIREX-AQ laboratory and field experiments may provide insight to these relationships.

Measurements of optical properties of smoke have been performed using chamber measurements (Hungershoefer et al., 2008), AERONET Sun photometer network observations (Sayer et al., 2014), and field observations (e.g., Haywood et al., 2003). Measurements were conducted under different environmental conditions, in different geographical regions, and by different techniques. A synthesis approach will need to be developed to establish consistent characterization of smoke optical properties as a function of burning and environmental conditions.

During the burning process, emitted trace gases may condense and form aerosols, in addition to particles that are directly emitted. Smoke particles are emitted into the atmosphere as an internal mixture of BC, organic material (OM), and other aerosol species (such as sulfates and nitrates). The BC component of smoke strongly absorbs solar radiation, while the other components, including OM, primarily scatter solar radiation—the “direct aerosol effect” of smoke (Hobbs et al., 1997). In the IPCC (2013) report, the net

global mean radiative forcing due to smoke-radiation interaction is small, but uncertain, -0.0 (-0.20 to $+0.20$) W/m^2 . Myhre et al. (2013) examined the RF-direct (direct radiative forcing) of smoke using AeroCom Phase II simulations and found that, in the boreal region, the zonal mean of the RF-direct from smoke is a small net cooling (AeroCom model mean $<0.05 \text{ W/m}^2$). However, during an extreme fire event, the local RF-direct can be large. For example, Péré et al. (2014) examined the direct radiative effect of the 2010 Russian wildfires and found that, over a large part of Eastern Europe, smoke aerosols significantly reduced the diurnal-averaged solar radiation at the ground by 80 – 150 W/m^2 . The net radiative effect of absorbing aerosols depends on the albedo of the underlying surface (Haywood & Shine, 1995), and at high latitudes, the RF-direct of smoke can switch from a cooling to a warming effect at the TOA, as the surface becomes covered in snow and ice (Stone et al., 2008).

Absorption of solar radiation by smoke can also result in local changes to cloud liquid water path and cloud fraction. Cloud responses to aerosol-induced atmospheric heating provide an additional influence on the radiation budget at the TOA and at the surface. These cloud responses, often referred to as the semidirect effect, are due to radiative interactions between aerosol and cloud and are distinguished from microphysical interactions (indirect effects), which are discussed in the next section. Impacts depend on the vertical distribution of the smoke, however, and several different mechanisms have been identified. Absorption by smoke located within the boundary layer can reduce cloud cover by reducing relative humidity and evaporating cloud droplets (Ackerman et al., 2000). Heating within smoke layers located above the boundary layer, and the associated cooling at the surface, tend to increase atmospheric stability and can inhibit entrainment at cloud top, leading to a moister boundary layer and increases in cloud liquid water path (LWP). There is observational evidence that heating within smoke layers above marine stratocumulus can lead to increases in cloud albedo and a net cooling effect (Wilcox, 2012). Combining observations with modeling, Sakaeda et al. (2011) found that aerosol-induced increases in atmospheric stability can also increase marine cloud cover, which has larger radiative impacts than the changes in LWP. On the other hand, over land they find the atmospheric heating and surface cooling from smoke aerosols tend to suppress convection and reduce surface evaporation and the vertical transport of moisture, leading to reduced cloud LWP but with minimal impacts on cloud fraction. Koch and Del Genio (2010) provide a useful review of the various mechanisms responsible for aerosol radiative influences on cloud cover.

Many studies on smoke-radiation interaction do not explicitly distinguish direct and semidirect effects (e.g., Ge et al., 2014; Tosca et al., 2010; Tosca et al., 2013). Tosca et al. (2010) ran the Community Atmosphere Model (CAM) and found that the direct and semidirect aerosol effects of smoke reduce the net shortwave radiation at the surface by 19.1 W/m^2 during August–October in Sumatra and Borneo, while the semidirect aerosol effect of smoke reduces the cloud fraction and precipitation. A study based on nine global coupled climate models found a global net cooling at TOA from the semidirect effect of BC, which significantly compensated for the warming of the direct effect, resulting in a net TOA radiative impact from anthropogenic BC of only 0.082 W/m^2 (Stjern et al., 2017). Therefore, proper evaluation of the impact of smoke on the global radiation budget requires consideration of the variety of mechanisms by which smoke interacts radiatively with clouds.

Even though UV radiation plays a key role in the environment and on human health, the impact of smoke on UV radiation remains largely unquantified. However, there are ongoing efforts to understand the integrated and often competing surface and atmospheric direct and indirect radiative effects of smoke. These include ongoing field campaigns (e.g., FIREX-AQ, CAMP2X) and model investigations focused on understanding these integrated, competing interactions. For instance, JL Ward et al. (2018) found that statistically significant snowmelt could occur over much of the Greenland Ice Sheet due to in-snow black carbon, yet in contrast, light-absorbing aerosols in the atmosphere were shown to substantially dampen the solar radiation absorbed by in-snow aerosols. Additionally, Park et al. (2018) pioneered an approach to model smoke impacts on UV radiation. A similar approach can be applied to compute the solar radiative impact, but the spectral optical properties of smoke across the solar spectrum will be required.

5. Smoke Impacts on Clouds and Precipitation

It has been known for some time that smoke particles originating from biomass burning can act as cloud condensation nuclei (CCN; Hobbs & Radke, 1969). In recent work, Zamora et al. (2016) estimated that the

smoke-driven cloud albedo effect could decrease local summertime shortwave radiation flux by 2 to 4 W m^{-2} in the Arctic and subarctic. The activation of cloud droplets from smoke particles directly depends on properties such as size distribution and chemical composition (Petters, Carrico, et al., 2009). For liquid-phase clouds with a given mass of water, smoke-contaminated clouds tend to have a higher cloud droplet number concentration (CDNC), smaller droplet sizes, and higher cloud albedo compared to smoke-free clouds (referred to as the “first indirect effect” or “cloud albedo effect”; Twomey, 1974). Smaller cloud drops may slow down the collision-coalescence rate and delay the onset of precipitation (referred to as the “second indirect effect” or “cloud lifetime effect”; Albrecht, 1989). The impacts on liquid-phase clouds of smoke particles acting as CCN have been confirmed by numerous observational and modeling studies (Graf et al., 2009; Langmann, 2007; Martins et al., 2009; Rosenfeld, 1999).

Andreae et al. (2004) and Rosenfeld et al. (2008) proposed the following mechanism by which smoke might affect convective clouds: more CCN activated from aerosol delay the formation of rain, and prolong the cloud lifetime. As a result, more ice-phase hydrometeors are formed at a higher altitude associated with a large amount of latent heat release. Hence, the convective clouds will become more vigorous. This effect is referred to as the “thermodynamic effect” by Lohmann and Feichter (2005). However, the strength, or even the sign, of this effect strongly depends on a variety of environmental parameters such as the convective available potential energy, relative humidity, and vertical wind shear (Fan et al., 2009; Khain et al., 2005). Several studies investigating aerosol influences on storms have found that aerosols (CCN) can either strengthen or weaken updrafts and downdrafts depending on the size and complexity of storms and the nature of their associated small-scale circulations, and thus influence storm development (S S Lee, 2011; Seifert & Beheng, 2006; Van Den Heever & Cotton, 2007).

Higher CCN concentrations can also affect another important ice-phase microphysical process: riming (collection of cloud droplets by falling snow). Borys et al. (2003) show that polluted clouds rime less efficiently because smaller cloud droplets are harder to collect. As a result, the formation of snow is suppressed, and the amount of precipitation is also reduced. This so-called “riming indirect effect” (Lohmann & Feichter, 2005) was observed, and also simulated in modeling studies (Lance et al., 2011; Saleeby et al., 2009). Morrison et al. (2008) conducted a sensitivity test and found that the size-dependent collection efficiency accounts for about one fourth to one half of the differences in the ice water path and precipitation rate due to aerosol pollution. Lu and Sokolik (2013) found that precipitation has a nonlinear response to the amount of smoke, mainly due to the riming indirect effect.

The impact of smoke on the riming process is poorly represented in the majority of mesoscale models as shown in Table 1. This poor representation is, to a great extent, due to our inadequate understanding of the ice-phase microphysical processes (Fridlind et al., 2007; IPCC, 2013) and is also partially due to the limitation of the one-moment microphysics scheme used in mesoscale models (e.g., the Lin microphysics scheme in WRF-Chem; Grell et al., 2011; Wu et al., 2011). In contrast, a two-moment microphysics scheme (e.g., the Morrison two-moment scheme (Morrison et al., 2005)) predicts both the number concentrations and the mixing ratios of hydrometeors; therefore, it allows the effective radius to evolve in a realistic manner, which is critical for several microphysical processes, including riming.

Vali (2014) suggested that the compositional influence on ice nucleation or the specific “ice nuclei” may be nebulous for internally mixed particles, and hence redefined particles possessing ice nucleating elements as ice nucleating particles (INPs). Prediction of direct smoke impact of INPs on clouds and precipitation is extremely challenging because understanding of emission rates and types of particles from fires capable of influencing ice formation as INPs is very limited. Analysis of INP compositions in free tropospheric air (P. J. DeMott et al., 2003) and from sampling ice crystal residuals (Cziczo et al., 2013; Kamphus et al., 2010) suggest that biomass burning contributions to global tropospheric INPs are modest, at perhaps less than 10% by number. However, indirect regional or larger-scale influence of biomass burning aerosols on ice formation have been inferred based on strong correlations between ice particle concentration, BC and INP concentrations present in orographic wave cloud residues (Twohy et al., 2010), and based on apparent ice formation-INP closure in clouds ingesting biomass burning aerosols thought to be from agricultural fires after long-range transport (Stith et al., 2011). At least one model-observation analysis (Phillips et al., 2013) supported the dominance of BC INPs (presumed from biomass burning) that was seen as correlations only in the observational studies (Eidhammer et al., 2010; Twohy et al., 2010). However, more recent laboratory data on BC

Table 1

Mesoscale Modeling Studies That Focus on the Impact of Smoke or Aerosols on Cloud Microphysical Processes (From Zheng, 2014)

Paper	Model	Region	Size and composition	Smoke's effect on liquid-phase process	Smoke's effect on ice-phase process
Martins et al. (2009)	BRAMS	Amazon	N/A	Fixed CCN	N/A
Graf et al. (2009)	REMOTE-CCFM	Indonesia	TPM	Empirical CCN activation	N/A
Grell et al. (2011)	WRF-Chem	Alaska	Yes (fixed σ); OM + BC	Prognostic CCN (ARG scheme ^b)	N/A
Wu et al. (2011)	WRF-Chem	Amazon	Yes (fixed σ); OM + BC	Prognostic CCN (ARG scheme)	N/A
Hoeve et al. (2012)	GATOR-GCMOM	Amazon	Yes; OM + BC	Prognostic CCN	PK97 IN scheme ^c
Morrison et al. (2008) ^a	MM5	Alaska	Prescribed aerosol	Diagnostic CCN (ARG scheme)	Size-dependent RCE ^d
Saleeby et al. (2009) ^a	RAMS	Colorado	Prescribed aerosol	Diagnostic CCN	Size-dependent RCE ^d
Seifert et al. (2012) ^a	COSMO-DE	Germany	Prescribed aerosol	Diagnostic CCN (look-up table)	P08 IN scheme ^e

^aThree studies consider general aerosols. ^bARG scheme: Abdul-Razzak and Ghan (2000). ^cPK97 IN scheme: Pruppacher and Klett (1997). ^dSize-dependent RCE: size-dependent Riming Collection Efficiency. ^eP08 IN scheme: Phillips et al. (2008).

INPs from biomass combustion (Levin et al., 2014; Levin et al., 2016) and fossil fuel combustion (Schill et al., 2016) do not support as strong a role as assumed in Phillips et al. (2013) for BC in general as an INP source in the combustion of a majority of biomass types for mixed-phase cloud conditions. This agrees with the relatively weak evidence for the activity of carbonaceous soot aerosols as INPs in most laboratory studies in the temperature regime higher than -38°C (Bond et al., 2013; Kanji et al., 2013). Clear evidence for soot INPs has been established by two methods (BC-removal prior to INP measurement and electron microscopy inspection of INPs) primarily for certain grasses (Levin et al., 2016; McCluskey et al., 2014).

There is presently no question that fire emissions are associated with direct production of immersion freezing INPs of varied strength for some fuels burned in the laboratory (Petters, Parsons, et al., 2009), and INP are detected directly in emissions from prescribed fires (Pratt et al., 2011; Prenni et al., 2012; Twohy et al., 2010). Support is also present from remote sensing studies of plume-cloud interactions (Sassen & Khvorostyanov, 2008). Nevertheless, the most comprehensive direct atmospheric observations of wildfire smoke as INPs thus far have come primarily from ground sites. These studies also quantified INP emissions as functions of total particle numbers and size (McCluskey et al., 2014; Prenni et al., 2012), but as yet, comprehensive parameterizations to describe emissions over the full mixed-phase cloud temperature range have not been developed. It can be expected that such INP emissions may be impacted by fire size, intensity, stage, fuel composition, degree of flaming versus smoldering combustion, and age. In addition to carbonaceous INP types (OM, BC), coarse-mode production of INPs from lofted soils, ash, and uncombusted plant material may make major contributions that are not well quantified, and may distinguish emissions between prescribed, agricultural, and natural fires (McCluskey et al., 2014). This is expected based on numerous studies indicating the lofting of such material in wildfires (e.g., Wagner et al., 2018). Hence, fire emissions of INPs may be immensely complicated, and thus, more *in situ* sampling is greatly needed.

Ice crystals formed from INPs can quickly glaciate supercooled cloud droplets via the Bergeron-Findeisen process, enhance the precipitation, and reduce the cloud lifetime, which is known as the “glaciation indirect effect” (Lohmann, 2002). Khain et al. (2008) speculate that primary ice nucleation plays a more important role in frontal clouds (as well as stratocumulus clouds) than in cumulus clouds in the Amazon. However, how smoke INPs affect the cloud microphysical properties and precipitation of convective mixed-phase clouds is still largely uncertain. By modeling a convective storm in Florida, Heever et al. (2006) found that the case with more INPs alone leads to a higher onset temperature for ice crystals and the largest surface rainfall as compared to other cases with high CCN. Seifert et al. (2012) found that an increase in the INP concentration results in decreased cloud water path because of higher freezing efficiency, and leads to more snow water path. However, the domain-averaged precipitation is relatively less affected.

Significant efforts have been focused on developing a more complex representation of microphysical processes with enhanced coupling to atmospheric aerosols (e.g., Gustafson et al., 2007; Saleeby et al., 2009; Yang et al., 2011). Table 1 reviews recent mesoscale modeling studies that couple microphysical processes with smoke properties (or general aerosols). The physically based coupling between smoke (the aerosol module) and clouds (the microphysics module) requires information on smoke size distribution, chemical composition, and mixing state. In Graf et al. (2009), smoke emissions are incorporated in the model as total

particulate matter (TPM); therefore, only the empirical relationship between smoke mass concentration and the CCN number concentration can be applied. In studies that employ the WRF-Chem model (Grell et al., 2005; Grell et al., 2011; Wu et al., 2011), smoke emissions are size- and composition-resolved. For example, the chemical composition of freshly emitted smoke particles is assumed to be a function of vegetation type; the size distribution of fresh smoke particles is prescribed with a fixed standard deviation σ . In addition, the WRF-Chem model is able to simulate additional processes (e.g., coagulation, dry/wet deposition) that are related to the evolution of smoke particles. Coupled with aerosol properties, the WRF-Chem model is able to calculate CCN activation using a physically based parameterization, the Abdul-Razzak and Ghan (ARG) scheme (2000) (e.g., in Gustafson et al., 2007), which was systematically evaluated in Ghan et al. (2011). Results reveal that the ARG scheme performs well under most common conditions compared to more complex parameterizations, such as the Nenes scheme (Fountoukis & Nenes, 2005).

Although the importance of INPs was discussed above, the majority of studies that focus on the smoke-cloud-precipitation interaction do not directly account for the INPs activated from smoke particles. Either the effect of INPs is not considered at all (Graf et al., 2009), or temperature-dependent ice nucleation parameterizations are employed (Ge et al., 2014; Grell et al., 2011; Langmann, 2007; Wu et al., 2011). Significant efforts have been devoted to the development of heterogeneous ice nucleating particle parameterizations, either through in situ measurement and laboratory experiments or through derivation of classical theory (Paul J DeMott et al., 2010; Hoose et al., 2008; Khvorostyanov & Curry, 2004; Lohmann & Diehl, 2006; Phillips et al., 2008). Parameterizations run the gamut, from fully parametric to multicomponent and time-dependent, to treat varied ice-nucleation mechanisms. These may be general to all INP types or more commonly are specific to particle compositions ranging from biological to soot to mineral and soil particles. Parsing out the specific contributions of OM and BC of relevance to wildfire INP emissions has only been attempted in one case (Phillips et al., 2008, 2013), but the specific applicability of tunable parameters has never been tested for wildfire plume conditions. In general, it can be stated that parameterization development specific to wildfire INP emissions must await additional measurements within plumes as a function of the many parameters that may determine the relevant compositions (OM, BC, dust, ash) of INPs.

6. Summary and Recommendations

Our goal has been to provide an introduction to this special issue and to provide a review of current fire-smoke emissions characterization, data, and modeling. There are several dominating themes that permeate this special issue and review that include the linkages and dependency of outcomes on ecosystem fuels (Desservet et al., 2017; Gomez et al., 2018; H Lee et al., 2018; X Liu et al., 2017; Petrenko et al., 2017, all this issue) and the interdependencies between the terrestrial, atmosphere, and climate domains (e.g., fuels, fire weather, detrainment and transport, chemistry, deposition of smoke, impacts on radiation, and precipitation; Antokhin et al., 2018; Bluvshtein et al., 2017; Kalashnikova et al., 2018; F. Li, et al., 2018; Lu & Sokolik, 2017; Souri et al., 2017; Wang et al., 2018; Zhu et al., 2017, all this issue). The ultimate purpose of understanding fire-smoke emissions, their properties, transport, and atmospheric impacts is twofold: to clarify chemistry and transport to improve air quality and health and to accurately integrate and model feedback within climatic systems.

In every section of this review, ecosystem fuels are characterized as a substantial contributor to the measurement or outcome. Section 3 characterizes smoke emission estimates, which are highly dependent on the amount of fuel contained in an ecosystem, fuel availability (dryness, consumption), and fire behavior, which are predominately under the control of climate and weather. There has been a disconnection between small-scale terrestrial fire models and large-scale atmospheric models, largely due to distinct spatial and temporal scales and dissimilar goals. Modelers of small-scale fire behavior at the surface are concerned with predicting fire direction, fire behavior, and spread rate for fire management or to gauge near-field air quality impacts in preparation for prescribed burns. The goal of large-scale modelers is to realistically track smoke, which is commonly transported in filaments at a range of altitudes, so emissions have to be unrealistically large to accurately represent concentrations on coarse model grids. Connecting these disparate communities that work on fundamentally different spatial scales, ranging from a field-based perspective of meters to a global atmospheric model perspective, is challenging. Section 5 demonstrates that a proper evaluation of the impact of smoke on the global radiation budget requires consideration of the variety of mechanisms by

which smoke interacts radiatively with clouds. The diverse radiative impacts of smoke are often competing and integrate direct and indirect effects that have proven difficult to assess. This is due to the large variability in smoke loading and properties, with a lack of direct connection to the sources of these differences. Furthermore, in section 6, recent literature demonstrates that smoke particles can serve as both CCN and INPs, depending on the smoke's chemical and physical properties, and atmospheric conditions. The ice-nucleating ability of particles found in smoke from biomass burning strongly varies with fuel type, fire behavior, and environmental conditions. However, measurements within plumes, as a function of the many parameters that may determine the relevant compositions, are limited. Current field campaigns are expected to provide insights.

To conclude this review, we present the following recommendations in hopes of ensuring advancement in the study of smoke from biomass burning and the integral and diverse feedback and impacts of smoke on air quality, human and ecosystem health, and climate.

- Amass the statistics necessary to explore the interconnected factors that drive smoke composition and chemistry, especially as these relate to the factors that connect terrestrial information to synoptic comprehension (e.g., fire behavior to FRP and to smoke detrainment; fuel type and fire weather to secondary chemistry and distant air quality);
- Work toward an interactive “cumulative effect” understanding of total fire emissions and integrate these in models, which would necessarily include (1) total fuel consumed (minimally—ecosystem type, determinate fire weather, and the concomitant fraction of flaming and smoldering) and (2) smoke's vertical and horizontal extent;
- Improve understanding and model parameterization of fire plume injection height and, perhaps even more importantly, smoke detrainment height, which drives transport and subsequent air quality, health, and climate impacts (e.g., radiation, precipitation). This would necessarily include statistics from numerous small- to medium-sized fires, and the parameterization of large and extreme fires (e.g., prescribed, agricultural, natural, feedback with clouds, pyro-cumulous, pyro-cumulonimbus);
- Consider satellite overpass times when analyzing data and also when considering the overpass times of future satellites. Bear in mind natural fires peak in the late afternoon, and cloud and smoke cover can inhibit fire detection and FRP strength;
- Improve model resolution and/or smoke filament modeling, while recognizing the purpose of each model drives its rationale. These improvements would result in increased accuracy and mass-balanced smoke emissions accounting;
- Establish a database of smoke particle shapes, as a function of size, as well as burning conditions, in order to significantly improve the understanding of smoke radiative impacts;
- Document field campaign data and make the data available to the broad scientific community without any restriction. Suggestions for complete data reporting include observing methodology that contains detection measurement and principles, instrument calibration method, and standards; assumptions and ancillary data used in data processing, sampling strategy, procedures, and treatment; instrument and/or measurement reference; measurement uncertainty estimate and estimate method; data variable description; and reporting conditions [e.g., Standard Temperature and Pressure (STP)]. Often this information is forgotten with time and is necessary to maintain data viability. These steps will greatly enhance the scientific return on the taxpayer money invested in conducting expensive field programs, as well as significantly enhance scientific credibility;
- Document results of radiative model calculations in a well-organized documented database. This should include data on spectral smoke optical properties, with the relevant information used for computation.
- Measurements are needed to represent all environmental conditions in which smoke particles may serve as CCN or/and INPs, ranging from northern latitude wildfires where boreal wildfires occur to tropical forest wildfires and from small agricultural/cropland fires to prescription fires. In addition, models should endeavor to take into account smoke particles serving as CCN and INPs in a variety of ecosystems under specific environmental conditions.
- Because fire emissions of INPs are immensely complicated, *in situ* sampling is greatly needed. Consequently, the development of wildfire INP emissions must await additional measurements within plumes as a function of the many parameters that may determine the relevant compositions (OM, BC, dust, ash) of INPs.

As an aid to readers, we provide links to the following helpful websites, which provided the data analyzed in this work:

Biomass burning emission in GEOS-Chem (links to other emissions too): http://wiki.seas.harvard.edu/geos-chem/index.php/Biomass_burning_emissions

CWFIS (Canadian Wildland Fire Information System): <http://cwfis.cfs.nrcan.gc.ca/home>

FINN (Fire Emissions from NCAR): <https://www2.acom.ucar.edu/modeling/finn-fire-inventory-ncar>

GFED data: <http://www.globalfiredata.org/>

ICARTT (International Consortium for Atmospheric Research on Transport and Transformation) Data Format Standard: <https://www-air.larc.nasa.gov/missions/etc/IcarttDataFormat.htm>

MODIS and VIIRS fire data: <https://earthdata.nasa.gov/earth-observation-data/near-real-time/firms>; <http://modis-fire.umd.edu/ba.html>

NASA FireChem Whitepaper: <https://espo.nasa.gov/sites/default/files/documents/FIREChem%20White%20Paper.pdf>; <https://www.esrl.noaa.gov/csd/projects/firex/>

NIFC (National Interagency Fire Center): <https://www.nifc.gov/>

VIIRS Data Record Updates: <https://viirsland.gsfc.nasa.gov/Products/NASA/NASAprod.html>

Acknowledgments

I.N. Sokolik acknowledges the support from NASA grant NNX16AH69G and NSF grant 1637279. A. Soja and D. Winker gratefully acknowledge the support that led to this work from the CloudSat and CALIPSO program and project NNX16AM30G. Soja is also greatly appreciative of a FIREChem award (80NSSC18K0685) that aids in supporting this research. P. DeMott acknowledges support from the NSF award 1650786.

References

Abdul-Razzak, H., & Ghan, S. J. (2000). A parameterization of aerosol activation: 2, Multiple aerosol types. *Journal of Geophysical Research - Atmospheres*, 105(D5), 6837–6844. <https://doi.org/10.1029/1999JD901161>

Ackerman, A. S., Toon, O., Stevens, D., Heymsfield, A., Ramanathan, V., & Welton, E. (2000). Reduction of tropical cloudiness by soot. *Science*, 288(5468), 1042–1047. <https://doi.org/10.1126/science.288.5468.1042>

Akagi, S. K., Yokelson, R. J., Wiedinmyer, C., Alvarado, M. J., Reid, J. S., Karl, T., et al. (2011). Emission factors for open and domestic biomass burning for use in atmospheric models. *Atmospheric Chemistry and Physics*, 11(9), 4039–4072. <https://doi.org/10.5194/acp-11-4039-2011>

Albrecht, B. A. (1989). Aerosols, Cloud Microphysics, and Fractional Cloudiness. *Science*, 245(4923), 1227–1230. <https://doi.org/10.1126/science.245.4923.1227>

Alexander, D. T., Crozier, P. A., & Anderson, J. R. (2008). Brown carbon spheres in East Asian outflow and their optical properties. *Science*, 321(5890), 833–836. <https://doi.org/10.1126/science.1155296>

Al-Saadi, J. (2009). Assessing satellite-based fire data for use in the National Emissions Inventory. *Journal of Applied Remote Sensing*, 3(031504), 29. <https://doi.org/10.1117/1.3148859>

Andela, N., Morton, D. C., Giglio, L., Chen, Y., van der Werf, G. R., Kasibhatla, P. S., et al. (2017). A human-driven decline in global burned area. *Science*, 356(6345), 1356–1362. <https://doi.org/10.1126/science.aa14108>

Andreae, M. O., & Merlet, P. (2001). Emission of trace gases and aerosols from biomass burning. *Global biogeochemical cycles*, 15, 955–966. <https://doi.org/10.1029/2000GB001382>

Andreae, M. O., Rosenfeld, D., Artaxo, P., Costa, A., Frank, G., Longo, K., & Silva-Dias, M. A. F. d. (2004). Smoking rain clouds over the Amazon. *Science*, 303(5662), 1337–1342. <https://doi.org/10.1126/science.1092779>

Antokhin, P. N., Arshinova, V. G., Arshinov, M. Y., Belan, B. D., Belan, S. B., Davydov, D. K., et al. (2018). Distribution of Trace Gases and Aerosols in the Troposphere Over Siberia During Wildfires of Summer 2012. *Journal of Geophysical Research: Atmospheres*, 123(4), 2285–2297. <https://doi.org/10.1002/2017jd026825>

Aragão, L. E. O. C., & Shimabukuro, Y. E. (2010). The Incidence of Fire in Amazonian Forests with Implications for REDD. *Science*, 328(5983), 1275–1278. <https://doi.org/10.1126/science.1186925>

Bluvshtein, N., Lin, P., Flores, J. M., Segev, L., Mazar, Y., Tas, E., et al. (2017). Broadband optical properties of biomass-burning aerosol and identification of brown carbon chromophores. *Journal of Geophysical Research: Atmospheres*, 122, 5441–5456. <https://doi.org/10.1002/2016jd026230>

Bond, T. C., Doherty, S. J., Fahey, D. W., Forster, P. M., Berntsen, T., DeAngelo, B. J., et al. (2013). Bounding the role of black carbon in the climate system: A scientific assessment. *Journal of Geophysical Research: Atmospheres*, 118, 5380–5552. <https://doi.org/10.1002/jgrd.50171>

Borys, R. D., Lowenthal, D. H., Cohn, S. A., & Brown, W. O. J. (2003). Mountaintop and radar measurements of anthropogenic aerosol effects on snow growth and snowfall rate. *Geophysical Research Letters*, 30(10), 1538. <https://doi.org/10.1029/2002GL016855>

Burton, S. P., Ferrare, R. A., Hostetler, C. A., Hair, J. W., Roger, R. R., Oblad, M. D., et al. (2012). Aerosol classification using airborne High Spectral Resolution Lidar measurements - methodology and examples. *Atmospheric Measurement Techniques*, 5, 73–98. <https://doi.org/10.5194/amt-5-73-2012>

Cahoon, D. R. Jr., Stocks, B. J., Levine, J. S., Cofer, W. R. III, & Chung, C. C. (1992). Evaluation of a technique for satellite-derived area estimation of forest-fires. *Journal of Geophysical Research*, 97(D4), 3805–3814. <https://doi.org/10.1029/91jd03080>

Cruz, M., Gould, J., Hollis, J., & McCaw, W. (2018). A Hierarchical classification of wildland fire fuels for Australian vegetation types. *Firehouse*, 1(1), 13. <https://doi.org/10.3390/fire1010013>

Cziczo, D. J., Froyd, K. D., Hoose, C., Jensen, E. J., Diao, M., Zondlo, M. A., et al. (2013). Clarifying the Dominant Sources and Mechanisms of Cirrus Cloud Formation. *Science*, 340(6138), 1320–1324. <https://doi.org/10.1126/science.1234145>

Damoah, R., Spichtinger, N. C., Forster, P. J., Mattis, I., Wandinger, U., Beirle, S., & Stohl, A. (2004). Around the world in 17 days - hemispheric-scale transport of forest fire smoke from Russia in May 2003. *Atmospheric Chemistry and Physics*, 4, 1311–1321. <https://doi.org/10.5194/acp-4-1311-2004>

DeMott, P. J., Cziczo, D. J., Prenni, A. J., Murphy, D. M., Kreidenweis, S. M., Thomson, D. S., et al. (2003). Measurements of the concentration and composition of nuclei for cirrus formation. *Proceedings of the National Academy of Sciences*, 100(25), 14,655–14,660. <https://doi.org/10.1073/pnas.2532677100>

DeMott, P. J., Prenni, A. J., Liu, X., Kreidenweis, S. M., Petters, M. D., Twohy, C. H., et al. (2010). Predicting global atmospheric ice nuclei distributions and their impacts on climate. *Proceedings of the National Academy of Sciences*, 107(25), 11,217–11,222. <https://doi.org/10.1073/pnas.0910818107>

Desservetaz, M., Paton-Walsh, C., Griffith, D. W. T., Kettlewell, G., Keywood, M. D., Vanderschoot, M. V., et al. (2017). Emission factors of trace gases and particles from tropical savanna fires in Australia. *Journal of Geophysical Research: Atmospheres*, 122, 6059–6074. <https://doi.org/10.1002/2016jd025925>

Dozier, J. (1981). A method for satellite identification of surface temperature fields of subpixel resolution. *Remote Sensing of Environment*, 11, 221–229. [https://doi.org/10.1016/0034-4257\(81\)90021-3](https://doi.org/10.1016/0034-4257(81)90021-3)

Duff, T., Keane, R., Penman, T., & Tolhurst, K. (2017). Revisiting wildland fire fuel quantification methods: the challenge of understanding a dynamic, biotic entity. *Forests*, 8(9), 351. <https://doi.org/10.3390/f8090351>

Eidhammer, T., DeMott, P., Prenni, A., Petters, M., Twohy, C., Rogers, D., et al. (2010). Ice initiation by aerosol particles: Measured and predicted ice nuclei concentrations versus measured ice crystal concentrations in an orographic wave cloud. *Journal of the Atmospheric Sciences*, 67(8), 2417–2436. <https://doi.org/10.1175/2010jas3266.1>

Fan, J., Yuan, T., Comstock, J. M., Ghan, S., Khain, A., Leung, L. R., et al. (2009). Dominant role by vertical wind shear in regulating aerosol effects on deep convective clouds. *Journal of Geophysical Research - Atmospheres*, 114(D22). <https://doi.org/10.1029/2009JD012352>

Flannigan, M. D., Krawchuk, M. A., de Groot, W. J., Wotton, B. M., & Gowman, L. M. (2009). Implications of changing climate for global wildland fire. *International Journal of Wildland Fire*, 18(5), 483–507. <https://doi.org/10.1071/wf08187>

Fountoukis, C., & Nenes, A. (2005). Continued development of a cloud droplet formation parameterization for global climate models. *Journal of Geophysical Research - Atmospheres*, 110(D11). <https://doi.org/10.1029/2004JD005591>

Freeborn, P. H., Wooster, M. J., & Roberts, G. (2011). Addressing the spatiotemporal sampling design of MODIS to provide estimates of the fire radiative energy emitted from Africa. *Remote Sensing of Environment*, 115(2), 475–489. <https://doi.org/10.1016/j.rse.2010.09.017>

Freitas, S. R., Longo, K. M., Chatfield, R., Latham, D., Silva Dias, M. A. F., Andreae, M. O., et al. (2007). Including the sub-grid scale plume rise of vegetation fires in low resolution atmospheric transport models. *Atmospheric Chemistry and Physics*, 7(13), 3385–3398. <https://doi.org/10.5194/acp-7-3385-2007>

Freitas, S. R., Longo, K. M., Silva Dias, M. A. F., Chatfield, R., Silva Dias, P., Artaxo, P., et al. (2009). The Coupled Aerosol and Tracer Transport model to the Brazilian developments on the Regional Atmospheric Modeling System (CATT-BRAMS) – Part 1: Model description and evaluation. *Atmospheric Chemistry and Physics*, 9(8), 2843–2861. <https://doi.org/10.5194/acp-9-2843-2009>

Fridlind, A. M., Ackerman, A. S., McFarquhar, G., Zhang, G., Poellot, M. R., DeMott, P. J., et al. (2007). Ice properties of single-layer stratocumulus during the Mixed-Phase Arctic Cloud Experiment: 2. Model results. *Journal of Geophysical Research - Atmospheres*, 112 (D24). <https://doi.org/10.1029/2007JD008646>

Fromm, M., Lindsey, D. T., Servranckx, R., Yue, G., Trickl, T., Sica, R., et al. (2010). The untold story of pyrocumulonimbus. *Bulletin of the American Meteorological Society*, American Meteorological Society, 91(9), 1193–1209. <https://doi.org/10.1175/2010BAMS3004.1>

Ge, C., Wang, J., & Reid, J. (2014). Mesoscale modeling of smoke transport over the Southeast Asian Maritime Continent: coupling of smoke direct radiative effect below and above the low-level clouds. *Atmospheric Chemistry and Physics*, 14(1), 159–174. <https://doi.org/10.5194/acp-14-159-2014>

Ghan, S. J., Abdul-Razzak, H., Nenes, A., Ming, Y., Liu, X., Ovchinnikov, M., et al. (2011). Droplet nucleation: Physically-based parameterizations and comparative evaluation. *Journal of Advances in Modeling Earth Systems*, 3, M10001. <https://doi.org/10.1029/2011MS000074>

Giglio, L., Descloitres, J., Justice, C. O., & Kaufman, Y. J. (2003). An enhanced contextual fire detection algorithm for MODIS. *Remote Sensing of Environment*, 87(2-3), 273–282. [https://doi.org/10.1016/s0034-4257\(03\)00184-6](https://doi.org/10.1016/s0034-4257(03)00184-6)

Giglio, L., Loboda, T., Roy, D. P., Quayle, B., & Justice, C. O. (2009). An active-fire based burned area mapping algorithm for the MODIS sensor. *Remote Sensing of Environment*, 113(2), 408–420. <https://doi.org/10.1016/j.rse.2008.10.006>

Giglio, L., Randerson, J. T., van der Werf, G. R., Kasibhatla, P. S., Collatz, G. J., Morton, D. C., & DeFries, R. S. (2010). Assessing variability and long-term trends in burned area by merging multiple satellite fire products. *Biogeosciences*, 7(3), 1171–1186. <https://doi.org/10.5194/bg-7-1171-2010>

Giglio, L., Schroeder, W., & Justice, C. O. (2016). The collection 6 MODIS active fire detection algorithm and fire products. *Remote Sensing of Environment*, 178, 31–41. <https://doi.org/10.1016/j.rse.2016.02.054>

Giglio, L., van der Werf, G. R., Randerson, J. T., Collatz, G. J., & Kasibhatla, P. (2006). Global estimation of burned area using MODIS active fire observations. *Atmospheric Chemistry and Physics*, 6(4), 957–974. <https://doi.org/10.5194/acp-6-957-2006>

Gomez, S. L., Carrico, C. M., Allen, C., Lam, J., Dabli, S., Sullivan, A. P., et al. (2018). Southwestern U.S., Biomass Burning Smoke Hygroscopicity: The Role of Plant Phenology, Chemical Composition, and Combustion Properties. *Journal of Geophysical Research: Atmospheres*, 123(10), 5416–5432. <https://doi.org/10.1029/2017jd028162>

Graf, H. F., Yang, J., & Wagner, T. M. (2009). Aerosol effects on clouds and precipitation during the 1997 smoke episode in Indonesia. *Atmospheric Chemistry and Physics*, 9(2), 743–756. <https://doi.org/10.5194/acp-9-743-2009>

Grell, G. A., Freitas, S., Stuefer, M., & Fast, J. (2011). Inclusion of biomass burning in WRF-Chem: impact of wildfires on weather forecasts. *Atmospheric Chemistry and Physics*, 11(11), 5289. <https://doi.org/10.5194/acp-11-5289-2011>

Grell, G. A., Peckham, S. E., Schmitz, R., McKeen, S. A., Frost, G., Skamarock, W. C., & Eder, B. (2005). Fully coupled "online" chemistry within the WRF model. *Atmospheric Environment*, 39(37), 6957–6975. <https://doi.org/10.1016/j.atmosenv.2005.04.027>

Gustafson, W. I., Chapman, E. G., Ghan, S. J., Easter, R. C., & Fast, J. D. (2007). Impact on modeled cloud characteristics due to simplified treatment of uniform cloud condensation nuclei during NEAQS 2004. *Geophysical Research Letters*, 34, L19809. <https://doi.org/10.1029/2007GL030021>

Haywood, J. M., Francis, P., Dubovik, O., Glew, M., & Holben, B. (2003). Comparison of aerosol size distributions, radiative properties, and optical depths determined by aircraft observations and Sun photometers during SAFARI 2000. *Journal of Geophysical Research - Atmospheres*, 108(D13). <https://doi.org/10.1029/2002jd002250>

Haywood, J. M., & Shine, K. P. (1995). The effect of anthropogenic sulfate and soot aerosol on the clear sky planetary radiation budget. *Geophysical Research Letters*, 22(5), 603–606. <https://doi.org/10.1029/95gl00075>

Heever, S. C. v. d., Carrión, G. G., Cotton, W. R., DeMott, P. J., & Prenni, A. J. (2006). Impacts of Nucleating Aerosol on Florida Storms. Part I: Mesoscale Simulations. *Journal of the Atmospheric Sciences*, 63(7), 1752–1775. <https://doi.org/10.1175/jas3713.1>

Hobbs, P. V., & Radke, L. (1969). Cloud condensation nuclei from a simulated forest fire. *Science*, 163(3864), 279–280. <https://doi.org/10.1126/science.163.3864.279>

Hobbs, P. V., Reid, J. S., Kotchenruther, R. A., Ferek, R. J., & Weiss, R. (1997). Direct Radiative Forcing by Smoke from Biomass Burning. *Science*, 275(5307), 1777–1778. <https://doi.org/10.1126/science.275.5307.1777>

Hoeve, J. E. T., Jacobson, M. Z., & Remer, L. A. (2012). Comparing results from a physical model with satellite and in situ observations to determine whether biomass burning aerosols over the Amazon brighten or burn off clouds. *Journal of Geophysical Research - Atmospheres*, 117(D8). <https://doi.org/10.1029/2011JD016856>

Hoose, C., Lohmann, U., Erdin, R., & Tegen, I. (2008). The global influence of dust mineralogical composition on heterogeneous ice nucleation in mixed-phase clouds. *Environmental Research Letters*, 3(2), 025003. <https://doi.org/10.1088/1748-9326/3/2/025003>

Hungrhoefer, K., Zeromskiene, K., Iinuma, Y., Helas, G., Trentmann, J., Trautmann, T., et al. (2008). Modelling the optical properties of fresh biomass burning aerosol produced in a smoke chamber: results from the EFEU campaign. *Atmospheric Chemistry and Physics*, 8(13), 3427–3439. <https://doi.org/10.5194/acp-8-3427-2008>

Ichoku, C., & Ellison, L. (2014). Global top-down smoke-aerosol emissions estimation using satellite fire radiative power measurements. *Atmospheric Chemistry and Physics*, 14(13), 6643–6667. <https://doi.org/10.5194/acp-14-6643-2014>

Ichoku, C., & Kaufman, Y. J. (2005). A method to derive smoke emission rates from MODIS fire radiative energy measurements. *IEEE Transactions on Geoscience and Remote Sensing*, 43(11), 2636–2649. <https://doi.org/10.1109/tgrs.2005.857328>

IPCC (2013). *Climate Change 2013: The Physical Science Basis. Contribution of Working Group I to the Fifth Assessment Report of the Intergovernmental Panel on Climate Change*, (p. 1535). Cambridge, United Kingdom and New York, NY, USA: Cambridge University Press. <https://doi.org/10.1017/CBO9781107415324>

Jolly, W. M., Cochrane, M. A., Freeborn, P. H., Holden, Z. A., Brown, T. J., Williamson, G. J., & Bowman, D. M. J. S. (2015). Climate-induced variations in global wildfire danger from 1979 to 2013. *Nature Communications*, 6, 7537. <https://doi.org/10.1038/ncomms8537>

Justice, C. O., Giglio, L., Korontzi, S., Owens, J., Morisette, J. T., Roy, D., et al. (2002). The MODIS fire products. *Remote Sensing of Environment*, 83(1-2). [https://doi.org/10.1016/S0034-4257\(02\)00076-00077](https://doi.org/10.1016/S0034-4257(02)00076-00077)

Kahn, R. A., Chen, Y., Nelson, D. L., Leung, F.-Y., Li, Q., Diner, D. J., & Logan, J. A. (2008). Wildfire smoke injection heights: Two perspectives from space. *Geophysical Research Letters*, 35, L04809. <https://doi.org/10.1029/2007GL032165>

Kahn, R. A., & Gaitley, B. J. (2015). An analysis of global aerosol type as retrieved by MISR. *Journal of Geophysical Research: Atmospheres*, 120, 4248–4281. <https://doi.org/10.1002/2015JD023322>

Kahn, R. A., Li, W.-H., Moroney, C., Diner, D. J., Martonchik, J. V., & Fishbein, E. (2007). Aerosol source plume physical characteristics from space-based multiangle imaging. *Journal of Geophysical Research*, 112, D11205. <https://doi.org/10.1029/2006JD007647>

Kaiser, J., Heil, A., Andreae, M., Benedetti, A., Chubarova, N., Jones, L., et al. (2012). Biomass burning emissions estimated with a global fire assimilation system based on observed fire radiative power. *Biogeosciences*, 9(1), 527. <https://doi.org/10.5194/bg-9-527-2012>

Kalashnikova, O. V., Garay, M. J., Bates, K. H., Kenseth, C. M., Kong, W., Cappa, C. D., et al. (2018). Photopolarimetric Sensitivity to Black Carbon Content of Wildfire Smoke: Results From the 2016 ImPACT-PM Field Campaign. *Journal of Geophysical Research: Atmospheres*, 123(10), 5376–5396. <https://doi.org/10.1029/2017jd028032>

Kamphus, M., Ettner-Mahl, M., Klimach, T., Drewnick, F., Keller, L., Cziczo, D. J., et al. (2010). Chemical composition of ambient aerosol, ice residues and cloud droplet residues in mixed-phase clouds: single particle analysis during the Cloud and Aerosol Characterization Experiment (CLACE 6). *Atmospheric Chemistry and Physics*, 10(16), 8077–8095. <https://doi.org/10.5194/acp-10-8077-2010>

Kanji, Z., Welti, A., Chou, C., Stetzer, O., & Lohmann, U. (2013). Laboratory studies of immersion and deposition mode ice nucleation of ozone aged mineral dust particles. *Atmospheric Chemistry and Physics*, 13(17), 9097–9118. <https://doi.org/10.5194/acp-13-9097-2013>

Kasischke, E. S., & Turetsky, M. R. (2006). Recent changes in the fire regime across the North American boreal region- spatial and temporal patterns of burning across Canada and Alaska. *Geophysical Research Letters*, 33, L09703. <https://doi.org/10.1029/2006GL025677>

Kaufman, Y. J., Justice, C. O., Flynn, L. P., Kendall, J. D., Prins, E. M., Giglio, L., et al. (1998). Potential global fire monitoring from EOS-MODIS. *Journal of Geophysical Research - Atmospheres*, 103(D24), 32,215–32,238. <https://doi.org/10.1029/98jd01644>

Kavouras, I. G., Nikolich, G., Etyemezian, V., DuBois, D. W., King, J., & Shafer, D. (2012). In situ observations of soil minerals and organic matter in the early phases of prescribed fires. *Journal of Geophysical Research - Atmospheres*, 117(D12). <https://doi.org/10.1029/2011jd017420>

Keegan, K. M., Albert, M. R., McConnell, J. R., & Baker, I. (2014). Climate change and forest fires synergistically drive widespread melt events of the Greenland Ice Sheet. *Proceedings of the National Academy of Sciences*, 111(22), 7964–7967. <https://doi.org/10.1073/pnas.1405397111>

Khain, A. P., BenMoshe, N., & Pokrovsky, A. (2008). Factors Determining the Impact of Aerosols on Surface Precipitation from Clouds: An Attempt at Classification. *Journal of the Atmospheric Sciences*, 65(6), 1721–1748. <https://doi.org/10.1175/2007jas2515.1>

Khain, A. P., Rosenfeld, D., & Pokrovsky, A. (2005). Aerosol impact on the dynamics and microphysics of deep convective clouds. *Quarterly Journal of the Royal Meteorological Society*, 131(611), 2639–2663. <https://doi.org/10.1256/qj.04.62>

Khvorostyanov, V. I., & Curry, J. A. (2004). The theory of ice nucleation by heterogeneous freezing of deliquescent mixed CCN. Part I: Critical radius, energy, and nucleation rate. *Journal of the Atmospheric Sciences*, 61(22), 2676–2691. <https://doi.org/10.1175/jas3266.1>

Koch, D., & Del Genio, A. (2010). Black carbon semi-direct effects on cloud cover: review and synthesis. *Atmospheric Chemistry and Physics*, 10(16), 7685–7696. <https://doi.org/10.5194/acp-10-7685-2010>

Kukavskaya, E. A., Soja, A. J., Petkov, A. P., Ponomarev, E. I., Ivanova, G. A., & Conard, S. G. (2012). Fire emissions estimates in Siberia: evaluation of uncertainties in area burned, land cover, and fuel consumption. *Canadian Journal of Forest Research*, 43(5), 493–506. <https://doi.org/10.1139/cjfr-2012-0367>

Lance, S., Shupe, M. D., Feingold, G., Brock, C. A., Cozic, J., Holloway, J. S., et al. (2011). Cloud condensation nuclei as a modulator of ice processes in Arctic mixed-phase clouds. *Atmospheric Chemistry and Physics*, 11(15), 8003–8015. <https://doi.org/10.5194/acp-11-8003-2011>

Langmann, B. (2007). A model study of smoke-haze influence on clouds and warm precipitation formation in Indonesia 1997/1998. *Atmospheric Environment*, 41(32), 6838–6852. <https://doi.org/10.1016/j.atmosenv.2007.04.050>

Langmann, B., Duncan, B., Textor, C., Trentmann, J., & van der Werf, G. R. (2009). Vegetation fire emissions and their impact on air pollution and climate. *Atmospheric Environment*, 43(1), 107–116. <https://doi.org/10.1016/j.atmosenv.2008.09.047>

Laskin, A., Laskin, J., & Nizkorodov, S. A. (2015). Chemistry of atmospheric brown carbon. *Chemical Reviews*, 115(10), 4335–4382. <https://doi.org/10.1021/cr5006167>

Lee, H., Jeong, S.-J., Kalashnikova, O., Tosca, M., Kim, S.-W., & Kug, J.-S. (2018). Characterization of Wildfire-Induced Aerosol Emissions From the Maritime Continent Peatland and Central African Dry Savannah with MISR and CALIPSO Aerosol Products. *Journal of Geophysical Research: Atmospheres*, 123(6), 3116–3125. <https://doi.org/10.1002/2017jd027415>

Lee, S. S. (2011). Dependence of aerosol-precipitation interactions on humidity in a multiple-cloud system. *Atmospheric Chemistry and Physics*, 11(5), 2179–2196. <https://doi.org/10.5194/acp-11-2179-2011>

Levin, E., McMeeking, G., DeMott, P., McCluskey, C., Carrico, C., Nakao, S., et al. (2016). Ice-nucleating particle emissions from biomass combustion and the potential importance of soot aerosol. *Journal of Geophysical Research: Atmospheres*, 121, 5888–5903. <https://doi.org/10.1002/2016jd024879>

Levin, E., McMeeking, G., DeMott, P., McCluskey, C., Stockwell, C., Yokelson, R., & Kreidenweis, S. (2014). A new method to determine the number concentrations of refractory black carbon ice nucleating particles. *Aerosol Science and Technology*, 48(12), 1264–1275. <https://doi.org/10.1080/02786826.2014.977843>

Li, F., Zhang, X., Kondragunta, S., & Csiszar, I. (2018). Comparison of Fire Radiative Power Estimates From VIIRS and MODIS Observations. *Journal of Geophysical Research: Atmospheres*, 123(9), 4545–4563. <https://doi.org/10.1029/2017jd027823>

Li, M., Wang, T., Xie, M., Li, S., Zhuang, B., Chen, P., et al. (2018). Agricultural Fire Impacts on Ozone Photochemistry Over the Yangtze River Delta Region, East China. *Journal of Geophysical Research: Atmospheres*, 123(12), 6605–6623. <https://doi.org/10.1029/2018jd028582>

Littell, J. S., McKenzie, D., Peterson, D. L., & Westerling, A. L. (2009). Climate and wildfire area burned in western US ecoregions, 1916–2003. *Ecological Applications*, 19(4), 1003–1021. <https://doi.org/10.1890/07-1183>

Liu, X., Huey, L. G., Yokelson, R. J., Selimovic, V., Simpson, I. J., Müller, M., et al. (2017). Airborne measurements of western U.S. wildfire emissions: Comparison with prescribed burning and air quality implications. *Journal of Geophysical Research: Atmospheres*, 122, 6108–6129. <https://doi.org/10.1002/2016jd026315>

Liu, Z., Winker, D., Omar, A., Vaughan, M., Kar, J., Trepte, C., et al. (2015). Evaluation of CALIOP 532 nm aerosol optical depth over opaque water clouds. *Atmospheric Chemistry and Physics*, 15(3), 1265–1288. <https://doi.org/10.5194/acp-15-1265-2015>

Liu, Z. Y., Vaughan, M., Winker, D., Kittaka, C., Getzewich, B., Kuehn, R., et al. (2009). The CALIPSO Lidar Cloud and Aerosol Discrimination: Version 2 Algorithm and Initial Assessment of Performance. *Journal of Atmospheric and Oceanic Technology*, 26(7), 1198–1213. <https://doi.org/10.1175/2009jtecha1229.1>

Loboda, T. V., Hoy, E. E., Giglio, L., & Kasischke, E. S. (2011). Mapping burned area in Alaska using MODIS data: a data limitations-driven modification to the regional burned area algorithm. *International Journal of Wildland Fire*, 20(4), 487–496. <https://doi.org/10.1071/WF10017>

Lohmann, U. (2002). A glaciation indirect aerosol effect caused by soot aerosols. *Geophysical Research Letters*, 29(4), 11-1. <https://doi.org/10.1029/2001gl014357>

Lohmann, U., & Diehl, K. (2006). Sensitivity studies of the importance of dust ice nuclei for the indirect aerosol effect on stratiform mixed-phase clouds. *Journal of the Atmospheric Sciences*, 63(3), 968–982. <https://doi.org/10.1175/jas3662.1>

Lohmann, U., & Feichter, J. (2005). Global indirect aerosol effects: a review. *Atmospheric Chemistry and Physics*, 5(3), 715–737. <https://doi.org/10.5194/acp-5-715-2005>

Lu, Z., & Sokolik, I. N. (2013). The effect of smoke emission amount on changes in cloud properties and precipitation: A case study of Canadian boreal wildfires of 2007. *Journal of Geophysical Research: Atmospheres*, 118, 11,777–11,793. <https://doi.org/10.1002/2013JD019860>

Lu, Z., & Sokolik, I. N. (2017). Examining the Impact of Smoke on Frontal Clouds and Precipitation During the 2002 Yakutsk Wildfires Using the WRF-Chem-SMOKE Model and Satellite Data. *Journal of Geophysical Research: Atmospheres*, 122, 12,765–712,785. <https://doi.org/10.1002/2017jd027001>

Mardi, A. H., Dadashazar, H., MacDonald, A. B., Braun, R. A., Crosbie, E., Xian, P., et al. (2018). Biomass Burning Plumes in the Vicinity of the California Coast: Airborne Characterization of Physicochemical Properties, Heating Rates, and Spatiotemporal Features. *Journal of Geophysical Research: Atmospheres*, 123(23), 13,560–13,582. <https://doi.org/10.1029/2018jd029134>

Martins, J. A., Silva Dias, M. A. F., & Gonçalves, F. L. T. (2009). Impact of biomass burning aerosols on precipitation in the Amazon: A modeling case study. *Journal of Geophysical Research - Atmospheres*, 114(D2). <https://doi.org/10.1029/2007JD009587>

Maudlin, L., Wang, Z., Jonsson, H., & Sorooshian, A. (2015). Impact of wildfires on size-resolved aerosol composition at a coastal California site. *Atmospheric Environment*, 119, 59–68. <https://doi.org/10.1016/j.atmosenv.2015.08.039>

McCluskey, C. S., DeMott, P. J., Prenni, A. J., Levin, E. J. T., McMeeking, G. R., Sullivan, A. P., et al. (2014). Characteristics of atmospheric ice nucleating particles associated with biomass burning in the US: Prescribed burns and wildfires. *Journal of Geophysical Research: Atmospheres*, 119, 10458–10470. <https://doi.org/10.1002/2014JD021980>

McKenzie, D., Raymond, C. L., Kellogg, L. K. B., Norheim, R. A., Andreu, A. G., Bayard, A. C., et al. (2007). Mapping fuels at multiple scales: landscape application of the Fuel Characteristic Classification SystemThis article is one of a selection of papers published in the Special Forum on the Fuel Characteristic Classification System. *Canadian Journal of Forest Research*, 37(12), 2421–2437. <https://doi.org/10.1139/X07-056>

Mhawish, A., Banerjee, T., Sorek-Hamer, M., Lyapustin, A., Broday, D. M., & Chatfield, R. (2019). Comparison and evaluation of MODIS Multi-angle Implementation of Atmospheric Correction (MAIAC) aerosol product over South Asia. *Remote Sensing of Environment*, 224, 12–28. <https://doi.org/10.1016/j.rse.2019.01.033>

Morrison, H., Curry, J. A., & Khvorostyanov, V. I. (2005). A New Double-Moment Microphysics Parameterization for Application in Cloud and Climate Models. Part I: Description. *Journal of the Atmospheric Sciences*, 62(6), 1665–1677. <https://doi.org/10.1175/jas3446.1>

Morrison, H., Pinto, J. O., Curry, J. A., & McFarquhar, G. M. (2008). Sensitivity of modeled arctic mixed-phase stratocumulus to cloud condensation and ice nuclei over regionally varying surface conditions. *Journal of Geophysical Research - Atmospheres*, 113(DS). <https://doi.org/10.1029/2007JD008729>

Myhre, G., Samset, B. H., Schulz, M., Balkanski, Y., Bauer, S., Berntsen, T. K., et al. (2013). Radiative forcing of the direct aerosol effect from AeroCom Phase II simulations. *Atmospheric Chemistry and Physics*, 13(4), 1853. <https://doi.org/10.5194/acp-13-1853-2013>

Natarajan, M., Pierce, R. B., Schaack, T. K., Lenzen, A. J., Al-Saadi, J. A., Soja, A. J., et al. (2012). Radiative forcing due to enhancements in tropospheric ozone and carbonaceous aerosols caused by Asian fires during spring 2008. *Journal of Geophysical Research*, 117(D6), D06307. <https://doi.org/10.1029/2011jd016584>

Omar, A. H., Winker, D. M., Vaughan, M. A., Hu, Y., Trepte, C. R., Ferrare, R. A., et al. (2009). The CALIPSO Automated Aerosol Classification and Lidar Ratio Selection Algorithm. *Journal of Atmospheric and Oceanic Technology*, 26(10), 1994–2014. <https://doi.org/10.1175/2009jtecha1231.1>

O'Neill, P. E., Lang, R. H., Kurum, M., Utiku, C., & Carver, K. R. (2006). Multi-Sensor Microwave Soil Moisture Remote Sensing: NASA's Combined Radar/Radiometer (ComRAD) System, paper presented at IEEE MicroRad, 2006, 0-0.

Park, Y. H., Sokolik, I. N., & Hall, S. R. (2018). The Impact of Smoke on the Ultraviolet and Visible Radiative Forcing Under Different Fire Regimes. *Air, Soil and Water Research*, 11, 1178622118774803. <https://doi.org/10.1177/1178622118774803>

Partain, J. L., Alden, S., Strader, H., Bhatt, U. S., Bieniek, P. A., Brettschneider, B. R., et al. (2016). An Assessment of the Role of Anthropogenic Climate Change in the Alaska Fire Season of 2015. *Bulletin of the American Meteorological Society*, 97(12), S14–S18. <https://doi.org/10.1175/bams-d-16-0149.1>

Pérez, J., Bessagnet, B., Mallet, M., Waquet, F., Chiapello, I., Minvielle, F., et al. (2014). Direct radiative effect of the Russian wildfires and its impact on air temperature and atmospheric dynamics during August 2010. *Atmospheric Chemistry and Physics*, 14(4), 1999–2013. <https://doi.org/10.5194/acp-14-1999-2014>

Peterson, D. A., Campbell, J., Hyer, E., Fromm, M., Kabilick, G., Cossuth, J., & DeLand, M. (2018). Wildfire-driven thunderstorms cause a volcano-like stratospheric injection of smoke. *Climate and Atmospheric Science*, 1, 30. <https://doi.org/10.1038/s41612-018-0039-3>

Peterson, D. A., Hyer, E. J., Campbell, J. R., Solbrig, J. E., & Fromm, M. D. (2017). A Conceptual Model for Development of Intense Pyrocumulonimbus in Western North America. *Monthly Weather Review*, 145(6), 2235–2255. <https://doi.org/10.1175/mwr-d-16-0232.1>

Petrenko, M., Kahn, R., Chin, M., & Limbacher, J. (2017). Refined Use of Satellite Aerosol Optical Depth Snapshots to Constrain Biomass Burning Emissions in the GOCART Model. *Journal of Geophysical Research: Atmospheres*, 122, 10,983–911,004. <https://doi.org/10.1002/2017jd026693>

Petrenko, M., Kahn, R., Chin, M., Soja, A. J., & Kucsera, T. (2012). The use of satellite-measured aerosol optical depth to constrain biomass burning emissions source strength in the global model GOCART. *Journal of Geophysical Research - Atmospheres*, 117(D18). <https://doi.org/10.1029/2012jd017870>

Petters, M. D., Carrico, C. M., Kreidenweis, S. M., Prenni, A. J., DeMott, P. J., Collett, J. L., & Moosmueller, H. (2009). Cloud condensation nucleation activity of biomass burning aerosol. *Journal of Geophysical Research - Atmospheres*, 114(D22). <https://doi.org/10.1029/2009jd012353>

Petters, M. D., Parsons, M. T., Prenni, A. J., DeMott, P. J., Kreidenweis, S. M., Carrico, C. M., et al. (2009). Ice nuclei emissions from biomass burning. *Journal of Geophysical Research - Atmospheres*, 114(D7). <https://doi.org/10.1029/2008JD011532>

Pfister, G. G., Hess, P. G., Emmons, L. K., Rasch, P. J., & Vitt, F. M. (2008). Impact of the summer 2004 Alaska fires on top of the atmosphere clear-sky radiation fluxes. *Journal of Geophysical Research - Atmospheres*, 113(D2). <https://doi.org/10.1029/2007JD008797>

Phillips, V. T., DeMott, P. J., & Andronache, C. (2008). An empirical parameterization of heterogeneous ice nucleation for multiple chemical species of aerosol. *Journal of the Atmospheric Sciences*, 65(9), 2757–2783. <https://doi.org/10.1175/2007jas2546.1>

Phillips, V. T., Demott, P. J., Andronache, C., Pratt, K. A., Prather, K. A., Subramanian, R., & Twohy, C. (2013). Improvements to an empirical parameterization of heterogeneous ice nucleation and its comparison with observations. *Journal of the Atmospheric Sciences*, 70(2), 378–409. <https://doi.org/10.1175/jas-d-12-080.1>

Pierce, R. B., Al-Saadi, J., Kittaka, C., Schaack, T., Lenzen, A., Bowman, K., et al. (2009). Impacts of background ozone production on Houston and Dallas, Texas, air quality during the Second Texas Air Quality Study field mission. *Journal of Geophysical Research-Atmospheres*, 114(D00F09). <https://doi.org/10.1029/2008JD011337>

Pierce, R. B., Schaack, T., Al-Saadi, J. A., Fairlie, T. D., Kittaka, C., Lingenfelter, G., et al. (2007). Chemical data assimilation estimates of continental U.S. ozone and nitrogen budgets during the Intercontinental Chemical Transport Experiment–North America. *Journal of Geophysical Research - Atmospheres*, 112(D12). <https://doi.org/10.1029/2006JD007722>

Polashenski, C. M., Dibb, J. E., Flanner, M. G., Chen, J. Y., Courville, Z. R., Lai, A. M., et al. (2015). Neither dust nor black carbon causing apparent albedo decline in Greenland's dry snow zone: Implications for MODIS C5 surface reflectance. *Geophysical Research Letters*, 42, 9319–9327. <https://doi.org/10.1002/2015GL065912>

Pratt, K. A., Murphy, S. M., Subramanian, R., DeMott, P. J., Kok, G. L., Campos, T., et al. (2011). Flight-based chemical characterization of biomass burning aerosols within two prescribed burn smoke plumes. *Atmospheric Chemistry and Physics*, 11(24), 12,549–12,565. <https://doi.org/10.5194/acp-11-12549-2011>

Prenni, A. J., DeMott, P. J., Sullivan, A. P., Sullivan, R. C., Kreidenweis, S. M., & Rogers, D. C. (2012). Biomass burning as a potential source for atmospheric ice nuclei: Western wildfires and prescribed burns. *Geophysical Research Letters*, 39, L11805. <https://doi.org/10.1029/2012GL051915>

Prins, E. M., Feltz, J. M., Menzel, W. P., & Ward, D. E. (1998). An overview of GOES-8 diurnal fire and smoke results for SCAR-B and 1995 fire season in South America. *Journal of Geophysical Research - Atmospheres*, 103(D24), 31,821–31,835. <https://doi.org/10.1029/98jd01720>

Prins, E. M., & Menzel, W. P. (1992). Geostationary satellite detection of bio mass burning in South America. *International Journal of Remote Sensing*, 13(15), 2783–2799. <https://doi.org/10.1080/01431169208904081>

Pruppacher, H. R., & Klett, J. D. (1997). *Microphysics of Clouds and Precipitation*. Dordrecht, The Netherlands: Kluwer Academic Publishers.

Raffuse, S. M., Craig, K. J., Larkin, N. K., Strand, T. T., Sullivan, D. C., Wheeler, N. J., & Solomon, R. (2012). An evaluation of modeled plume injection height with satellite-derived observed plume height. *Atmosphere*, 3(1), 103–123. <https://doi.org/10.3390/atmos3010103>

Randerson, J., Chen, Y., Werf, G., Rogers, B., & Morton, D. (2012). Global burned area and biomass burning emissions from small fires. *Journal of Geophysical Research - Biogeosciences*, 117(G4). <https://doi.org/10.1029/2012jg002128>

Rappold, A. G., Stone, S. L., Cascio, W. E., Neas, L. M., Kilaru, V. J., Caraway, M. S., et al. (2011). Peat Bog Wildfire Smoke Exposure in Rural North Carolina Is Associated with Cardiopulmonary Emergency Department Visits Assessed through Syndromic Surveillance. *Environmental Health Perspectives*, 119(10), 1415–1420. <https://doi.org/10.1289/ehp.1003206>

Reid, J. S., Hyer, E. J., Prins, E. M., Westphal, D. L., Zhang, J., Wang, J., et al. (2009). Global monitoring and forecasting of biomass-burning smoke: Description of and lessons from the Fire Locating and Modeling of Burning Emissions (FLAMBE) program. *IEEE Journal of Selected Topics in Applied Earth Observations and Remote Sensing*, 2(3), 144–162. <https://doi.org/10.1109/jstARS.2009.2027443>

Roberts, G., Wooster, M., Freeborn, P., & Xu, W. (2011). Integration of geostationary FRP and polar-orbiting burned area datasets for an enhanced biomass burning inventory. *Remote Sensing of Environment*, 115(8), 2047–2061. <https://doi.org/10.1016/j.rse.2011.04.006>

Rogers, R. R., Vaughan, M., Hostetler, C., Burton, S., Ferrare, R., Young, S., et al. (2014). Looking through the haze: evaluating the CALIPSO level 2 aerosol optical depth using airborne high spectral resolution lidar data. *Atmospheric Measurement Techniques*, 7(12), 4317–4340. <https://doi.org/10.5194/amt-7-4317-2014>

Rosenfeld, D. (1999). TRMM observed first direct evidence of smoke from forest fires inhibiting rainfall. *Geophysical Research Letters*, 26(20), 3105–3108. <https://doi.org/10.1029/1999GL006066>

Rosenfeld, D., Lohmann, U., Raga, G. B., O'Dowd, C. D., Kulmala, M., Fuzzi, S., et al. (2008). Flood or Drought: How Do Aerosols Affect Precipitation? *Science*, 321(5894), 1309–1313. <https://doi.org/10.1126/science.1160606>

Roy, D. P., Boschetti, L., Justice, C. O., & Ju, J. (2008). The Collection 5 MODIS Burned Area Product - Global Evaluation by Comparison with the MODIS Active Fire Product. *Remote Sensing of Environment*, 112(9), 3690–3707. <https://doi.org/10.1016/j.rse.2008.3605.3013>

Roy, D. P., Jin, Y., Lewis, P. E., & Justice, C. O. (2005). Prototyping a global algorithm for systematic fire-affected area mapping using MODIS time series data. *Remote Sensing of Environment*, 97(2), 137–162. <https://doi.org/10.1016/j.rse.2005.04.007>

Sakaeda, N., Wood, R., & Rasch, P. J. (2011). Direct and semidirect aerosol effects of southern African biomass burning aerosol. *Journal of Geophysical Research - Atmospheres*, 116(D12). <https://doi.org/10.1029/2010jd015540>

Saleebey, S. M., Cotton, W. R., Lowenthal, D., Borys, R. D., & Wetzel, M. A. (2009). Influence of Cloud Condensation Nuclei on Orographic Snowfall. *Journal of Applied Meteorology and Climatology*, 48(5), 903–922. <https://doi.org/10.1175/2008jamc1989.1>

Sassen, K., & Khorostyanov, V. I. (2008). Cloud effects from boreal forest fire smoke: Evidence for ice nucleation from polarization lidar data and cloud model simulations. *Environmental Research Letters*, 3(2), 025006. <https://doi.org/10.1088/1748-9326/3/2/025006>

Sayer, A. M., Hsu, N. C., Eck, T. F., Smirnov, A., & Holben, B. N. (2014). AERONET-based models of smoke-dominated aerosol near source regions and transported over oceans, and implications for satellite retrievals of aerosol optical depth. *Atmospheric Chemistry and Physics*, 14(20), 11,493–11,523. <https://doi.org/10.5194/acp-14-11493-2014>

Schill, G., Jathar, S., Kodros, J., Levin, E., Galang, A., Friedman, B., et al. (2016). Ice-nucleating particle emissions from photochemically aged diesel and biodiesel exhaust. *Geophysical Research Letters*, 43, 5524–5531. <https://doi.org/10.1002/2016gl069529>

Schlosser, J. S., Braun, R. A., Bradley, T., Dadashazar, H., MacDonald, A. B., Aldhaif, A. A., et al. (2017). Analysis of aerosol composition data for western United States wildfires between 2005 and 2015: Dust emissions, chloride depletion, and most enhanced aerosol constituents. *Journal of Geophysical Research: Atmospheres*, 122, 8951–8966. <https://doi.org/10.1002/2017jd026547>

Schmidt, I. B., Moura, L. C., Ferreira, M. C., Eloy, L., Sampaio, A. B., Dias, P. A., et al. (2018). Fire management in the Brazilian savanna: First steps and the way forward. *Journal of Applied Ecology*, 55(5), 2094–2101. <https://doi.org/10.1111/1365-2664.13118>

Schroeder, W., Oliva, P., Giglio, L., & Csiszar, I. A. (2014). The New VIIRS 375 m active fire detection data product: Algorithm description and initial assessment. *Remote Sensing of Environment*, 143, 85–96. <https://doi.org/10.1016/j.rse.2013.12.008>

Seifert, A., & Beheng, K. D. (2006). A two-moment cloud microphysics parameterization for mixed-phase clouds. Part 2: Maritime vs. continental deep convective storms. *Meteorology and Atmospheric Physics*, 92(1), 67–82. <https://doi.org/10.1007/s00703-005-0113-3>

Seifert, A., Köhler, C., & Beheng, K. D. (2012). Aerosol-cloud-precipitation effects over Germany as simulated by a convective-scale numerical weather prediction model. *Atmospheric Chemistry and Physics*, 12(2), 709–725. <https://doi.org/10.5194/acp-12-709-2012>

Seiler, W., & Crutzen, P. J. (1980). Estimates of gross and net fluxes of carbon between the biosphere and the atmosphere from biomass burning. *Climatic Change*, 2(3), 207–247. <https://doi.org/10.1007/bf00137988>

Sessions, W., Fuelberg, H., Kahn, R., & Winker, D. (2011). An investigation of methods for injecting emissions from boreal wildfires using WRF-Chem during ARCTAS. *Atmospheric Chemistry and Physics*, 11(12), 5719–5744. <https://doi.org/10.5194/acp-11-5719-2011>

Sheridan, P., Andrews, E., Ogren, J. A., Tackett, J., & Winker, D. (2012). Vertical profiles of aerosol optical properties over central Illinois and comparison with surface and satellite measurements. *Atmospheric Chemistry and Physics*, 12(23), 11,695–11,721. <https://doi.org/10.5194/acp-12-11695-2012>

Smith, W. L., & Rao P. K. (1971). The determination of surface temperature from satellite "window" radiation measurements, paper presented at Fifth Symposium on Temperature, Instrument Society of America, Washington, D.C., 21–24 June.

Sofiev, M., Vankevich, R., Lotjonen, M., Prank, M., Petukhov, V., Ermakova, T., et al. (2009). An operational system for the assimilation of the satellite information on wild-land fires for the needs of air quality modelling and forecasting. *Atmospheric Chemistry and Physics*, 9 (18), 6833–6847. <https://doi.org/10.5194/acp-9-6833-2009>

Soja, A. J., Cofer, W. R., Shugart, H. H., Sukhinin, A. I., Stackhouse, P. W., McRae, D. J., & Conard, S. G. (2004). Estimating fire emissions and disparities in boreal Siberia (1998–2002). *Journal of Geophysical Research*, 109(D14). <https://doi.org/10.1029/2004jd004570>

Soja, A. J., Fairlie, D., Westberg, D., Pouliot, G., & Szykman, J. (2012). *Biomass Burning Plume Injection Height Estimates using CALIOP, MODIS and the NASA Langley Trajectory Model*, paper presented at Environmental Protection Agency (EPA) International Emission Inventory Conference (EIC) Emission Inventories - Meeting the Challenges Posed by Emerging Global. Tampa Fl.: National, Regional and Local Air Quality Issues.

Soja, A. J., Tchekakova, N. M., French, N. H. F., Flannigan, M. D., Shugart, H. H., Stocks, B. J., et al. (2007). Climate-induced boreal forest change: Predictions versus current observations. *Global and Planetary Change, Special NEESPI Issue*, 56(3–4), 274–296. <https://doi.org/10.1016/j.gloplacha.2006.1007.1028>

Souri, A. H., Choi, Y., Jeon, W., Kochanski, A. K., Diao, L., Mandel, J., et al. (2017). Quantifying the Impact of Biomass Burning Emissions on Major Inorganic Aerosols and Their Precursors in the U. S. *Journal of Geophysical Research: Atmospheres*, 122, 12,020–012,041. <https://doi.org/10.1002/2017jd026788>

Stith, J. L., Twomey, C. H., DeMott, P. J., Baumgardner, D., Campos, T., Gao, R., & Anderson, J. (2011). Observations of ice nuclei and heterogeneous freezing in a Western Pacific extratropical storm. *Atmospheric Chemistry and Physics*, 11(13), 6229–6243. <https://doi.org/10.5194/acp-11-6229-2011>

Stjern, C. W., Samset, B. H., Myhre, G., Forster, P. M., Hodnebrog, Ø., Andrews, T., et al. (2017). Rapid adjustments cause weak surface temperature response to increased black carbon concentrations. *Journal of Geophysical Research: Atmospheres*, 122, 11–462. <https://doi.org/10.1002/2017jd027326>

Stocks, B. J., Fosberg, M. A., Lynham, T. J., Mearns, L., Wotton, B. M., Yang, Q., et al. (1998). Climate change and forest fire potential in Russian and Canadian boreal forests. *Climatic Change*, 38(1), 1–13. <https://doi.org/10.1023/a:1005306001055>

Stone, R. S., Anderson, G. P., Shettle, E. P., Andrews, E., Loukachine, K., Dutton, E. G., et al. (2008). Radiative impact of boreal smoke in the Arctic: Observed and modeled. *Journal of Geophysical Research*, 113(D14), D14S16. <https://doi.org/10.1029/2007jd009657>

Thomas, J. L., Polashenski, C. M., Soja, A. J., Marelle, L., Casey, K. A., Choi, H. D., et al. (2017). Quantifying black carbon deposition over the Greenland ice sheet from forest fires in Canada. *Geophysical Research Letters*, 44, 7965–7974. <https://doi.org/10.1002/2017GL073701>

Tosca, M. G., Randerson, J., & Zender, C. (2013). Global impact of smoke aerosols from landscape fires on climate and the Hadley circulation. *Atmospheric Chemistry and Physics*, 13(10), 5227–5241. <https://doi.org/10.5194/acp-13-5227-2013>

Tosca, M. G., Randerson, J. T., Zender, C. S., Flanner, M. G., & Rasch, P. J. (2010). Do biomass burning aerosols intensify drought in equatorial Asia during El Niño? *Atmospheric Chemistry and Physics*, 10(8), 3515–3528. <https://doi.org/10.5194/acp-10-3515-2010>

Twomey, C. H., DeMott, P. J., Pratt, K. A., Subramanian, R., Kok, G. L., Murphy, S. M., et al. (2010). Relationships of Biomass-Burning Aerosols to Ice in Orographic Wave Clouds. *Journal of the Atmospheric Sciences*, 67(8), 2437–2450. <https://doi.org/10.1175/2010jas3310.1>

Twomey, S. (1974). Pollution and the planetary albedo. *Atmospheric Environment* (1967), 8(12), 1251–1256. [https://doi.org/10.1016/0004-6981\(74\)90004-3](https://doi.org/10.1016/0004-6981(74)90004-3)

Val Martin, M., Kahn, R. A., Logan, J. A., Paugam, R., Wooster, M., & Ichoku, C. (2012). Space-based observational constraints for 1-D fire smoke plume-rise models. *Journal of Geophysical Research - Atmospheres*, 117(D22). <https://doi.org/10.1029/2012JD018370>

Van Den Heever, S. C., & Cotton, W. R. (2007). Urban aerosol impacts on downwind convective storms. *Journal of Applied Meteorology and Climatology*, 46(6), 828–850. <https://doi.org/10.1175/jam2492.1>

van der Werf, G. R., Randerson, J. T., Giglio, L., van Leeuwen, T. T., Chen, Y., Rogers, B. M., et al. (2017). Global fire emissions estimates during 1997–2015. *Earth System Science Data Discussions*, 2017, 1–43. <https://doi.org/10.5194/essd-2016-62>

Wang, J., Christopher, S. A., Nair, U., Reid, J. S., Prins, E. M., Szykman, J., & Hand, J. L. (2006). Mesoscale modeling of Central American smoke transport to the United States: 1. "Top-down" assessment of emission strength and diurnal variation impacts. *Journal of Geophysical Research*, 111, D05S17. <https://doi.org/10.1029/2005JD006416>

Wang, J., Yue, Y., Wang, Y., Ichoku, C., Ellison, L., & Zeng, J. (2018). Mitigating Satellite-Based Fire Sampling Limitations in Deriving Biomass Burning Emission Rates: Application to WRF-Chem Model Over the Northern sub-Saharan African Region. *Journal of Geophysical Research: Atmospheres*, 123(1), 507–528. <https://doi.org/10.1002/2017jd026840>

Ward, D. S., Kloster, S., Mahowald, N., Rogers, B., Randerson, J., & Hess, P. (2012). The changing radiative forcing of fires: global model estimates for past, present and future. *Atmospheric Chemistry and Physics*, 12(22), 10,857–10,886. <https://doi.org/10.5194/acp-12-10857-2012>

Ward, J. L., Flanner, M. G., Bergin, M., Dibb, J. E., Polashenski, C. M., Soja, A. J., & Thomas, J. L. (2018). Modeled Response of Greenland Snowmelt to the Presence of Biomass Burning-Based Absorbing Aerosols in the Atmosphere and Snow. *Journal of Geophysical Research: Atmospheres*, 123(11), 6122–6141. <https://doi.org/10.1029/2017JD027878>

Westerling, A. L., Hidalgo, H. G., Cayan, D. R., & Swetnam, T. W. (2006). Warming and earlier spring increase western US forest wildfire activity. *Science*, 313(5789), 940–943. <https://doi.org/10.1126/science.1128834>

Wiedinmyer, C., Akagi, S., Yokelson, R. J., Emmons, L., Al-Saadi, J., Orlando, J., & Soja, A. J. (2011). The Fire INventory from NCAR (FINN): a high resolution global model to estimate the emissions from open burning. *Geoscientific Model Development*, 4(3), 625. <https://doi.org/10.5194/gmd-4-625-2011>

Wilcox, E. M. (2012). Direct and semi-direct radiative forcing of smoke aerosols over clouds. *Atmospheric Chemistry and Physics*, 12(1), 139–149. <https://doi.org/10.5194/acp-12-139-2012>

Winker, D. M., Pelon, J., Coakley, J. A., Ackerman, S. A., Charlson, R. J., Colarco, P. R., et al. (2010). The CALIPSO Mission: A Global 3D View of Aerosols and Clouds. *Bulletin of the American Meteorological Society*, 91(9), 1211–1229. <https://doi.org/10.1175/2010bams3009.1>

Writter, S. (2015). *Heat wave, drought, wildfires in Russia (Summer 2010): MR Touch Natural hazards –Event reportRep*. RE, Münchener Rückversicherungs-Gesellschaft, GeoRisks Research, NatCatSERVICE: Munich.

Wu, L., Su, H., & Jiang, J. H. (2011). Regional simulations of deep convection and biomass burning over South America: 2. Biomass burning aerosol effects on clouds and precipitation. *Journal of Geophysical Research - Atmospheres*, 116(D17). <https://doi.org/10.1029/2011jd016106>

Yang, Q., Gustafson, W. Jr., Fast, J. D., Wang, H., Easter, R. C., Morrison, H., et al. (2011). Assessing regional scale predictions of aerosols, marine stratocumulus, and their interactions during VOCALS-REx using WRF-Chem. *Atmospheric Chemistry and Physics*, 11(23), 11951–11975. <https://doi.org/10.5194/acp-11-11951-2011>

Zamora, L. M., Kahn, R., Cubison, M. J., Diskin, G., Jimenez, J., Kondo, Y., et al. (2016). Aircraft-measured indirect cloud effects from biomass burning smoke in the Arctic and subarctic. *Atmospheric Chemistry and Physics*, 16(2), 715–738. <https://doi.org/10.5194/acp-16-715-2016>

Zhang, T., Wooster, M., de Jong, M., & Xu, W. (2018). How Well Does the 'Small Fire Boost' Methodology Used within the GFED4.1s Fire Emissions Database Represent the Timing, Location and Magnitude of Agricultural Burning? *Remote Sensing*, 10(6), 823. <https://doi.org/10.3390/rs10060823>

Zhang, X., Kondragunta, S., & Quayle, B. (2011). Estimation of biomass burned areas using multiple-satellite-observed active fires. *IEEE Transactions on Geoscience and Remote Sensing*, 49(11), 4469–4482. <https://doi.org/10.1109/tgrs.2011.2149535>

Zheng, L. (2014). *Examining the impact of wildfire smoke aerosol on clouds, precipitation, and radiative fluxes in Northern America and Russia using a fully coupled meso-scale model WRF-Chem-SMOKE and satellite data*. Ph.D. thesis. Atlanta, GA: Georgia Institute of Technology.

Zhu, J., Xia, X., Wang, J., Zhang, J., Wiedinmyer, C., Fisher, J. A., & Keller, C. A. (2017). Impact of Southeast Asian smoke on aerosol properties in Southwest China: First comparison of model simulations with satellite and ground observations. *Journal of Geophysical Research: Atmospheres*, 122, 3904–3919. <https://doi.org/10.1002/2016jd025793>